Lawrence Berkeley National Laboratory
Recent Work

Title
ILLUSTRATIONS OF A DENSITY-EQUALIZING MAP PROJECTION TECHNIQUE

Permalink
https://escholarship.org/uc/item/5vv516xs

Author
Selvin, S.

Publication Date
1987-04-01

eScholarship.org Powered by the California Digital Library
University of California

LBL-23189
c.2

Lawrence Berkeley Laboratory
UNIVERSITY OF CALIFORNIA, BERKELEY

Information and Computing Sciences Division

RECEIVED
LAWRENCE
BERKELEY LABORATORY
JUN 26 1987
LIBRARY AND
DOCUMENTS SECTION

ILLUSTRATIONS OF A DENSITY-EQUALIZING MAP PROJECTION TECHNIQUE

S. Selvin, D. Merrill, J. Schulman,
G. Shaw, W. Benson, and M. Mohr

April 1987

TWO-WEEK LOAN COPY

This is a Library Circulating Copy which may be borrowed for two weeks.

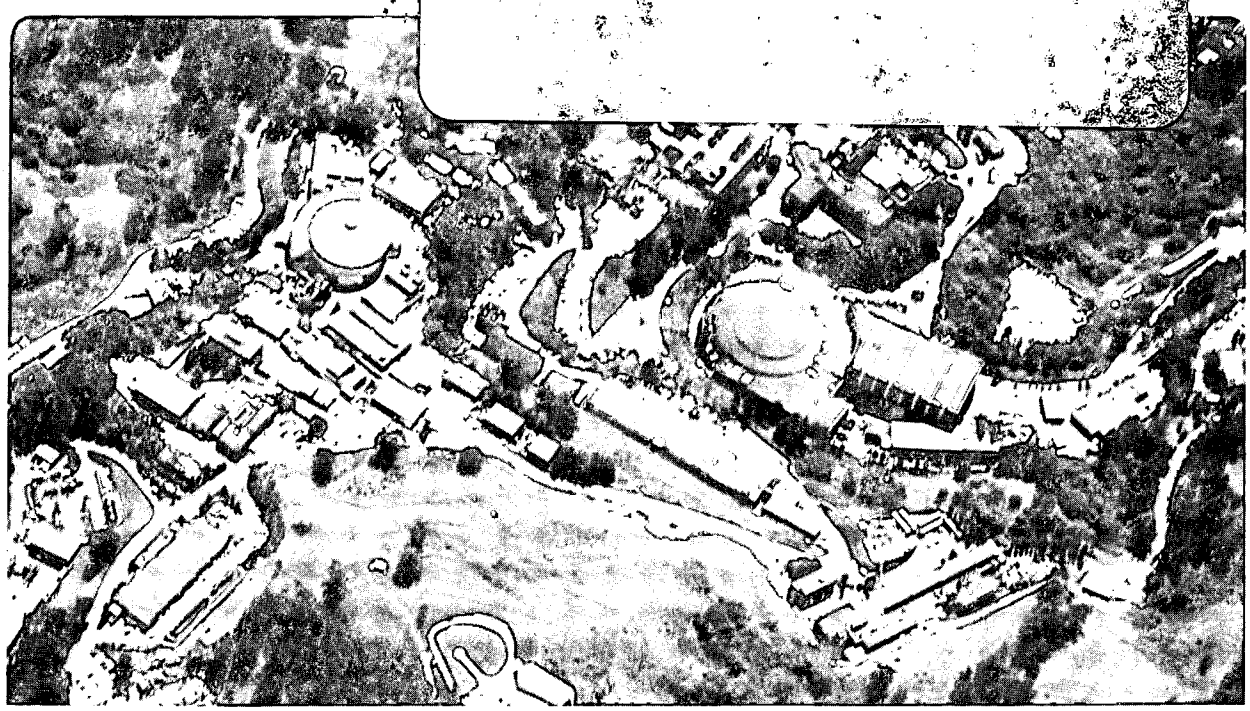

Prepared for the U.S. Department of Energy under Contract DE-AC03-76SF00098

LBL-23189
c.2

DISCLAIMER

This document was prepared as an account of work sponsored by the United States Government. While this document is believed to contain correct information, neither the United States Government nor any agency thereof, nor the Regents of the University of California, nor any of their employees, makes any warranty, express or implied, or assumes any legal responsibility for the accuracy, completeness, or usefulness of any information, apparatus, product, or process disclosed, or represents that its use would not infringe privately owned rights. Reference herein to any specific commercial product, process, or service by its trade name, trademark, manufacturer, or otherwise, does not necessarily constitute or imply its endorsement, recommendation, or favoring by the United States Government or any agency thereof, or the Regents of the University of California. The views and opinions of authors expressed herein do not necessarily state or reflect those of the United States Government or any agency thereof or the Regents of the University of California.

LBL-23189

ILLUSTRATIONS OF A DENSITY-EQUALIZING MAP PROJECTION TECHNIQUE

S.Selvin†‡; D.Merrill†‡; J.Schulman§; G.Shaw§; W.Benson†; and M.Mohr†‡

†Computer Science Research Department
Lawrence Berkeley Laboratory
University of California
Berkeley, California 94720

‡Department of Biostatistics
University of California
Berkeley, CA 94720

§California Birth Defects Monitoring Program
2980 Adeline Way
Berkeley, CA 94705

April, 1987

This research was supported by the Director, Office of Energy Research, Office of Health and Environmental Research of the U.S. Department of Energy under contract DE-AC03-76SF00098.

LBL-23189

ILLUSTRATIONS OF A DENSITY-EQUALIZING MAP PROJECTION TECHNIQUE

April 1987

Selvin, S.[1,2], Merrill, D.[1,2], Schulman, J.[3], Shaw, G.[3], Benson, W.[1], and Mohr, M.[1,2]

1. Computer Science Research Department, Lawrence Berkeley Laboratory, Berkeley, California 94720
2. Department of Biostatistics, University of California, Berkeley, California 94720
3. present address: California Birth Defects Monitoring Program, 2980 Adeline Way, Berkeley, California 94705.

Prepared for the U.S. Department of Energy under Contract DE-AC03-76SF00098

ABSTRACT

In attempting to analyze geographic clusters of disease, one is obliged to take account of varying population density. Customary methods, for example calculation of rates for subregions, are unsatisfactory: if subregions are too large, geographic detail is lost; if too small, stable rates cannot be calculated. In either case, adjacency relationships among cases are not easily analyzed. The usual difficulties are avoided by using an innovative projection technique. On a transformed map, population density is equalized while preserving adjacency relationships, so that clusters of cases can be easily recognized and their statistical significance measured. In this paper a density-equalizing computer algorithm is briefly described, and its use illustrated in representative applications.

KEYWORDS

computer mapping; cartogram; density-equalizing projection; disease clusters; population density; statistical analysis; spatial analysis; statistical geography; computer algorithm.

INTRODUCTION

The investigation of the spatial distribution of cases of disease is at the roots of epidemiology. In the nineteenth century John Snow discovered the source of cholera by plotting cases on a map of London. Others investigators have also made important contributions to the understanding of the disease process by simply noting that cases were distributed in some sort of a pattern over a specific region.

A fundamental problem associated with exploring the spatial distribution of a disease is the non-uniform distribution of human populations in most geographic regions. That is, humans tend to concentrate in specific areas, causing high frequency of disease to be necessarily associated with high densities of population, regardless of other factors that may influence the disease under study. One method of depicting the spatial distribution of disease, without the interfering influence of the non-uniform distribution of the population at risk, involves redrawing the geopolitical boundaries of a map. Such maps are commonly called cartograms. A cartogram can no longer be interpreted

in terms of geographical distance but has a distinct advantage in certain applications.

For the study of the spatial distribution of disease, a map must be constructed so that the population "at risk" is uniformly distributed. Figures 1 and 2 show an early attempt to depict the spatial distribution of smallpox while, at the same time, adjusting the map for the non-uniform "at risk" population of the state of California. If every individual in a given population has the same probability of contracting a disease, then cases of that disease, plotted on a cartogram where population density has been equalized, will be uniformly distributed on the transformed map. In other words, no statistically significant clusters of that disease will occur; such a situation can be rigorously tested with simple statistical procedures.

The California map in Figure 2 was produced via an arbitrary transformation of the county boundaries [1]. More recently, at Lawrence Berkeley Laboratory, a computerized radial transformation algorithm has been developed which can transform any geopolitical map to have equal density of population, or of any other selected variable.

ALGORITHM

We illustrate the density-equalizing algorithm in Figure 3, which shows the simplest possible case. On the left, the circle A and the doughnut-shaped region B have equal populations but unequal areas (A=10 and B=20). On the right, A and B have been radially transformed to give A' and B' the same area (A'=20 and B'=20) and hence the same population density. Note that the transformation changes the *area* but not the *shape* of A, and it changes the *shape* but not the *area* of B. (B' is a "skinnier" doughnut than B).

In the simple case shown, the necessary changes to the radii are easily calculated. With no essential differences, the same type of radial transformation can be applied to figures of any shape, not merely circles. In Figure 4 we illustrate the transformation for two irregularly shaped figures. The area of the inner figure is to be multiplied by a factor M while holding constant the area of the outer doughnut-shaped figure.

An arbitrary expansion center is defined within the inner figure; in an arbitrary direction a small-angle sector is defined which spans an angle θ, and covers an area A of the inner figure and an area B of the outer figure. For a small angle θ, A and B can be approximately expressed in terms of θ and R_1 and R_2, the distances from the expansion center to the boundary of the inner and outer figure respectively. The relationships are given on the left side of Figure 4.

On the right side of Figure 4, the area A is multiplied by a factor M to give a new area A'. The change is accomplished by changing R_1 to R_1' without changing θ. In order to keep area B' the same as B, R_2 is changed to a new value R_2'. The expressions for A' and B' in terms of θ, R_1' and R_2' appear in the top right part of Figure 4. From the expressions for A, B, A', and B', one obtains expressions for R_1' and R_2' that depend only on R_1 and R_2 and the magnification factor M; these expressions appear in the bottom right part of Figure 4. Of course R_1' and R_2', as well as R_1 and R_2, depend upon the arbitrary placement of the expansion center, and the arbitrary direction of the small-angle sector.

Now the same transformation is applied to every point i on the entire map. The locations of cases of disease and, optionally, latitude-longitude grid points are carried along in the process. The transformed distances R_1' and R_2' define a transformed inner figure whose area is M times as large as the original, and one or more transformed outer figures whose areas are all unchanged. In each case R_2 is the length of a straight line connecting point i with the chosen expansion center, and R_1 is the distance at which that line intersects the boundary of the inner figure.

Depending on the configuration of the inner figure, its expansion center, and the direction of the straight line to the point i being transformed, the line may intersect the boundary of the inner figure n times, at distances we call R_{11},R_{12},...R_{1n} (in order proceeding outward from the expansion center). In Figure 4 the expansion center lies inside the inner figure and all boundary points i of the outer figure lie outside, so the straight line always intersects the inner boundary just once (n = 1). More generally, R_1 is correctly defined as follows:

(a) expansion center inside, point i outside, n odd: $R_1^2 = +R_{11}^2-R_{12}^2+R_{13}^2-...+R_{1n}^2$

(b) expansion center inside, point i inside, n even: $R_1^2 = +R_{11}^2-R_{12}^2+R_{13}^2-...-R_{1n}^2+R_2^2$

(c) expansion center outside, point i outside, n even: $R_1^2 = -R_{11}^2+R_{12}^2-R_{13}^2+...+R_{1n}^2$

(d) expansion center outside, point i inside, n odd: $R_1^2 = -R_{11}^2+R_{12}^2-R_{13}^2+...-R_{1n}^2+R_2^2$

Finally, the necessary magnification is applied in turn to every figure in the entire map. Given figures $A,B,C...$ one first changes the area of A without changing the areas of $B,C,...$; then one changes the area of B without changing the areas of $A,C,...$; and so on. The magnification of figure A is taken to be

$$M_A=\frac{pop_A/pop_{total}}{area_A/area_{total}}$$

with corresponding expressions for M_B, M_C, etc. This choice gives a final map which has the same area $area_{total}$ as the original map.

The choice of an expansion center for each figure, and the order in which one expands (or contracts) the figures, are arbitrary. All possible choices yield final areas A', B',C',... proportional to pop_A,pop_B,pop_C,... and preserve the original adjacency relationships among the figures. It is shown elsewhere that if $A,B,C,...$ individually have uniform population density, then $A',B',C',...$ also have uniform population density, which implies uniform population density over the entire transformed map [2].

Any plane (Cartesian) projection is suitable as a starting point in the analysis; the quantities $area_A$ and $area_{total}$ indicate area as measured in that projection. In the density-equalizing process the shapes of all the figures are changed; spatial distortion appears to be minimized if the geographic centroid of each figure is chosen as its expansion center, and if the figures requiring the greatest relative change in area are processed first. In theory the area transformation is exact if each figure is described by infinitely many boundary points; in practice the precision of the result is subject to computer limitations. It is conjectured that a unique transformation with minimum distortion would result from an infinite number of infinitesimal transformations, using an infinite number of expansion centers uniformly distributed over the entire map; but this is a practical impossibility and is not required for the applications of interest.

An efficient implementation of the density-equalizing algorithm is a challenging problem in numerical computation, beyond the scope of this paper. A preliminary version has been tested on hardware ranging from an IBM PC to a Cray supercomputer. It is faster than the only other known implementation of a density-equalizing algorithm [3], but is still prohibitively slow for maps larger than a few thousand points. Each of the following examples required about an hour of computation on a DEC VAX-11/780 minicomputer. Work is continuing to improve the present implementation and to make it generally available.

EXAMPLES

Figure 5 shows a transformation applied to the United States, which equalizes 1980 population density. Similarly, Figure 6 shows transformations of the state of Iowa. The top figure is a typical geopolitical representation of Iowa, the middle figure is an hand-drawn cartogram [4], and the bottom figure is a computer-generated radial transformation.

SAN FRANCISCO COUNTY

Figures 7, 8 and 9 illustrate application of density-equalizing transformations to the 150 census tracts of the city/county of San Francisco. Figure 7 is a standard geopolitical representation of the 1980 census tracts with selected census tracts variously shaded (see figure caption). In Figure 8 the same map has been transformed to yield equal population density for white males 35 to 54 years of age. Note that the areas of high density (dotted shading) are expanded, and areas of low population density are decreased. Two areas, namely Golden Gate Park (the long rectangular area in the west) and a strictly industrial tract in the extreme southeastern corner, completely disappear because both have no permanent residents and are not relevant to population-related phenomena. Comparison of the areas having the solid shading (in Figure 8) shows the influence of the map transformation on predominantly black neighborhoods when adjusted for the white population only. Figure 9 is the result of the same process, except that the population used to produce the density-equalized map was the black male population 35 to 54 years of age. A fundamental point to notice is that after the map has been transformed, the interior boundaries are no longer relevant to the spatial distribution of cases of disease. For the maps of San Francisco the census tract boundaries are no longer of interest, because the entire transformed map now has the same population density.

Figure 10 shows 12 cases of a hypothetical "disease" with a rate of 26 cases per 100,000 population among white women ages 35 to 54, plotted by location on the geopolitical map of San Francisco. All women in San Francisco were assumed to be at exactly equal risk, and a random selection produced the 13 cases of "disease" shown in Figure 10. The density-equalized map is given in Figure 11. As expected under the hypothesis that every woman at risk has the same probability of contracting the "disease", no defined pattern emerges when "cases" are plotted on a transformed map.

Although analytic techniques have changed enormously since the time of John Snow, the essence is the same. Cases identified as occurring in proximity are considered as an indication of the existence of a common risk factor. Such a finding may help to better understand a disease process or at least provide clues for designing additional investigations. The study of spatial distributions provides basic information, particularly when specific environmental agents are suspected risk factors. Admittedly, the occurrences of most diseases are the combined result of a large number of complex factors that are not easily separated. Nevertheless, an excellent starting point for further exploration of the issues surrounding any disease is a careful and rigorous investigation of its spatial distribution. The remaining figures in this report represent observed disease distributions and illustrate how density-equalized maps can be used to identify non-random patterns of disease if and when they exist.

Figures 12 and 13 show, on density-equalized maps, the spatial distributions of stomach and colon cancers, as representative results from the analysis of cancer incidence in the city/county of San Francisco. In each figure a circle is plotted which is located at the centroid of the cases and which contains 50% of the cases observed. These circles serve as a visual tool to summarize both the location and dispersion of the cases of disease. For both cancers, the circles are large and centered near the population centroid of San Francisco, indicating no remarkable non-uniformity of the spatial distributions. A rigorous statistical analysis of the San Francisco data is described elsewhere [5].

CONTRA COSTA COUNTY

Lung cancer in Contra Costa county (CA) illustrates of the use of density-equalized maps to explore the relationship between the distribution of a specific disease and the location of a number of sources of potentially dangerous pollution. Previous investigators have noted the high frequency of lung cancers in the northern part of Contra Costa county, where five oil refineries are located (see Figure 14). A series of transformed maps was produced and the distance was measured from each case to the nearest plant. Figures 14 and 15 are examples of the maps used to calculate these distances. A complete statistical analysis is described elsewhere [6]. Although the transformed maps cases show a definite shift toward these refineries for some types of cancers, detailed interpretation of results is difficult. As mentioned, a spatial distribution is an excellent starting point for exploring a disease process, but is no more definitive than any analysis that considers only two variables out of the many complex influences involved in the phenomenon under study. The issues surrounding the observed excess of lung cancer in northern Contra Costa county have been extensively discussed (*e.g.* [7]) and the transformed maps demonstrate that the associations observed in the past continue to exist in more recent data.

SANTA CLARA COUNTY

Santa Clara county (CA) is another situation where density-equalized maps were employed to study the spatial distribution of a disease potentially associated with an environmental pollutant. In 1981 several chemical solvents were detected in the drinking water supplied to a portion of Santa Clara county (Figures 16 and 17). Reports of this contamination generated a number of health concerns, one of which was a possible increase in the frequency of cardiac defects among newborn infants [8]. With data collected for the years 1981 and 1982, transformed maps were employed to investigate a possibly non-random spatial distribution of cardiac defect cases in the county. For these two years every birth with a cardiac defect was plotted on a transformed map (Figure 17). Figures 17 and 18 show some of the results from this study. In the Santa Clara county study it was also possible to study a control group. That is, a series of normal births was collected and also plotted on the transformed maps. Figure 18 shows the centroids of the cases and these controls for both years. The distance between these two centroids is no larger than that expected by chance variation, implying that no strong geographic influence differentially affects the distribution of normal births and births with cardiac defects. (See [6] for a detailed description and analysis). A different approach, based on an *a priori* determination of the exposed region, shows some indication of clustering associated with the polluted water supply [9]. The difference in the conclusions drawn from the case/control approach and this alternative method apparently lies with the increase in statistical power achieved by identifying a specific area of exposure.

DENVER/JEFFERSON COUNTIES

In another example, we consider a plant producing components for nuclear weapons located in Jefferson county (CO) 16 miles northwest of the city of Denver, which is one of the nation's top producers of plutonium. Due to the extensive use of plutonium, the Rocky Flats facility has been the subject of several epidemiologic investigations concerning the possibility of an excess of lung cancers (*e.g.* [10,11]). Figures 19-30 show some of the results from statistical analysis of density-equalized map projections [6,2]. The spatial distribution of lung cancer cases from the Third National Cancer Survey (1970) in Denver and Jefferson counties was studied with particular reference to the Rocky Flats plant (location shown in Figure 19). The basic question addressed was whether the average distance of lung cancer cases to the Rocky Flats plant was smaller than might be expected from chance variation. These analyses were carried out on a large number of subpopulations defined by sex, age and histologic lung cancer type. Visually these transformed maps indicate that only random distributions of lung cancer cases are occurring in the Jefferson/Denver county area and, specifically, no association is observed with the Rocky Flats plant. This visual

impression is supported by extensive and rigorous statistical analysis of the lung cancer data (see [2]). For example, density functions describing the average minimum and maximum distances from a sample of cases to the Rocky Flats plant can be estimated and used in the statistical analyses (Figures 29 and 30).

CONCLUSIONS

A projection technique which transforms geopolitical maps so as to equalize the density of population at risk has important epidemiological applications. The most important advantage is that on a density-equalized map, geographic subdivisions of the study area, which have no inherent epidemiological significance, can be ignored. One need not calculate rates for individual subregions; such rates are generally unstable due to very small numbers of cases. The density-equalizing projection preserves the original adjacency relationships among cases, permitting supposed clusters of cases to be easily recognized and their statistical significance measured.

REFERENCES

1. J. W. Wallace. Population map for health officers. Am. J. Public Health. 1926; 16(10):1023.

2. J. Schulman. The statistical analysis of density-equalized map projections. Ph.D thesis. November 1986; LBL-22446.

3. W. Tobler, University of California at Santa Barbara; private communication.

4. A. G. Dean. Population based spot maps: an epidemiologic technique. Am. J. Public Health. 1976; 66(10):988-989.

5. S. Selvin, D. Merrill, S. Sacks, L. Wong, L. Bedell, and J. Schulman. Transformations of maps to investigate clusters of disease. October 1984; LBL-18550.

6. S. Selvin, G. Shaw, J. Schulman, and D. Merrill. Spatial distribution of disease: three case studies. August 1986 (submitted for publication).

7. J. Kaldor, J. Harris, E. Glazer, S. Glaser, R. Neutra, R. Mayberry, V. Nelson, L. Robinson, and D. Reed. Statistical association between cancer incidence and major-cause mortality, and estimated residential exposure to emissions from petroleum and chemical plants. Env. Hlt. Perspectives. 1984; 54:319-332.

8. Pregnancy outcomes in Santa Clara county 1980-1982: reports of two epidemiologic studies. Prepared by the California State Department of Health, Berkeley, CA.

9. G. Shaw, S. Selvin, S. Swan, D. Merrill, and J. Schulman. An empirical comparison of three disease clustering methodologies. August 1986; LBL-21162 (submitted for publication).

10. C. J. Johnson. Cancer incidence in an area contaminated with radionuclides near a nuclear installation. Ambio. 1981; 10(4):176-182.

11. P. W. Krey. Remote plutonium contamination and total inventories from Rocky Flats. Health Physics. 1976; 30:209-214.

INTRODUCTION

FIGURE 1
The distribution of smallpox cases in California (1915-1924) displayed on a geopolitical map [1].
FIGURE 2
One of the first attempts to depict the distribution of a disease and at the same time remove the confounding influence of varying population density.

ALGORITHM

FIGURE 3
A radial transformation applied to the simplest case of two areas labeled A and B, producing equalized densities for areas labeled A' and B'.
FIGURE 4
A radial transformation applied to areas A and B, which are sectors enclosed within a small angle θ, of two irregularly shaped areas. The transformation produces equalized densities for areas labeled A' and B'.

EXAMPLES

FIGURE 5
Illustration of a radial transformation applied to a geopolitical map of the United States (above). The transformed map (below) equalizes 1980 population density.
FIGURE 6
The state of Iowa: (i) a geopolitical map, (ii) map transformed to have equal population density (an arbitrary transformation drawn by hand) [4], and (iii) a density-equalized map projection resulting from a computer-generated radial transformation.

SAN FRANCISCO COUNTY

FIGURE 7
A geopolitical map showing 1980 Census tracts in the city/county of San Francisco. Dotted tracts = high density of white males ages 35-54; solid black tracts = high density of black males ages 35-54; striped tracts = small residential population.
FIGURE 8
Density-equalized map projection of San Francisco city/county, based on white male population of ages 35-54 (1980 Census). Dotted tracts = high density of white males ages 35-54; solid black tracts = high density of black males ages 35-54; striped tracts = small residential population.
FIGURE 9
Density-equalized map projection of San Francisco city/county, based on black male population of ages 35-54 (1980 Census). Solid black tracts = high density of black males ages 35-54; striped tracts = small residential population.
FIGURE 10
A geopolitical representation of San Francisco city/county with 13 cases of a hypothetical uniformly distributed disease (squares).
FIGURE 11
A density-equalized map projection of San Francisco city/county with 13 cases of a hypothetical uniformly distributed disease (squares).
FIGURE 12
A density-equalized map projection of San Francisco city/county, with 23 cases of colon cancer (squares) among white females aged 35 to 54, for the years 1978-1981. The circle is centered on the centroid of the cases and contains 50% of the cases.

FIGURE 13

A density-equalized map projection of San Francisco city/county, with 6 cases of stomach cancer (squares) among white females aged 35 to 54, for the years 1978-1981. The circle is centered on the centroid of the cases and contains 50% of the cases.

CONTRA COSTA COUNTY

FIGURE 14

A geopolitical map of Contra Costa county with the positions of five oil refineries indicated by circles.

FIGURE 15

Six transformed maps of Contra Costra county, showing the spatial distribution of lung cancer for white males and females aged 35-54, from 1979-1981 cancer incidence data.

SANTA CLARA COUNTY

FIGURE 16

A geopolitical map of Santa Clara county (excluding one large and sparsely populated census tract). Also shown is an area of high water pollution (shaded).

FIGURE 17

Cardiac defect cases and corresponding controls (live births) plotted on a density-equalized map projection of Santa Clara county for the years 1981-82. Also shown (outlined in the southeast corner of the county) is an area of high pollution of the county water system -- a potential source of this birth defect.

FIGURE 18

A density-equalized map showing the distance between the centroids of the cardiac defect cases and corresponding controls, for 1981 and 1982 data from Santa Clara county.

DENVER/JEFFERSON COUNTIES

FIGURE 19

A geopolitical map of Jefferson and Denver counties, Colorado. The location of the Rocky Flats plutonium processing facility is indicated by a small circle near the northern border.

FIGURE 20

The locations of cases of disease plotted on a geopolitical map (untransformed) and on a density-equalized map (based on 1970 Census population).

FIGURE 21

A geopolitical map of Jefferson and Denver counties, showing the spatial distribution of lung cancer (Adenocarcinoma) cases among white females over 55 years old, for the years 1969 through 1971.

FIGURE 22

A density-equalized map of Jefferson and Denver counties, showing the spatial distribution of lung cancer (Adenocarcinoma) cases among white females over 55 years old, for the years 1969 through 1971.

FIGURE 23

A geopolitical map of Jefferson and Denver counties, showing the spatial distribution of lung cancer (Small cell) cases among white females over 55 years old, for the years 1969 through 1971.

FIGURE 24

A density-equalized map of Jefferson and Denver counties, showing the spatial distribution of lung cancer (Small cell) cases among white females over 55 years old, for the years 1969 through 1971.

FIGURE 25

A density-equalized map of Jefferson and Denver counties, showing the spatial distribution of

leukemia cases among white males aged 35 to 54, for the years 1969 through 1971.

FIGURE 26

A density-equalized map of Jefferson and Denver counties, showing the spatial distribution of leukemia cases among white males over 55 years old, for the years 1969 through 1971.

FIGURE 27

A density-equalized map of Jefferson and Denver counties, showing the spatial distribution of leukemia cases among white females ages 35 to 54, for the years 1969 through 1971.

FIGURE 28

A density-equalized map of Jefferson and Denver counties, showing the spatial distribution of leukemia cases among white females over 55 years old, for the years 1969 through 1971.

FIGURE 29

Estimated density function of the average minimum distance from the Rocky Flats plant to a case of disease, as measured on a density-equalized map (sample size = 20).

FIGURE 30

Estimated density function of the average maximum distance from the Rocky Flats plant to a case of disease, as measured on a density-equalized map (sample size = 20).

Figure 1

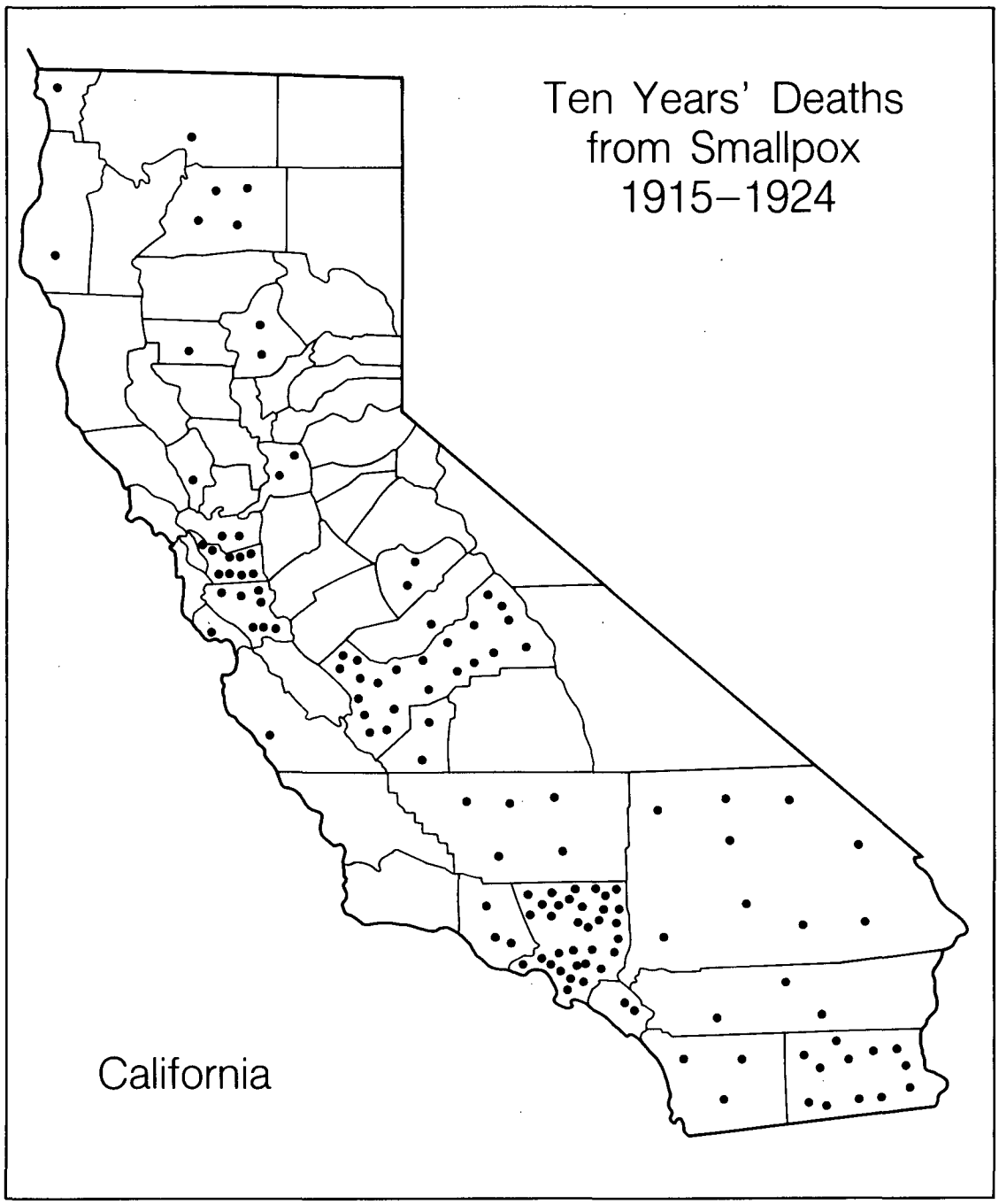

XBL 871-9806

Figure 2

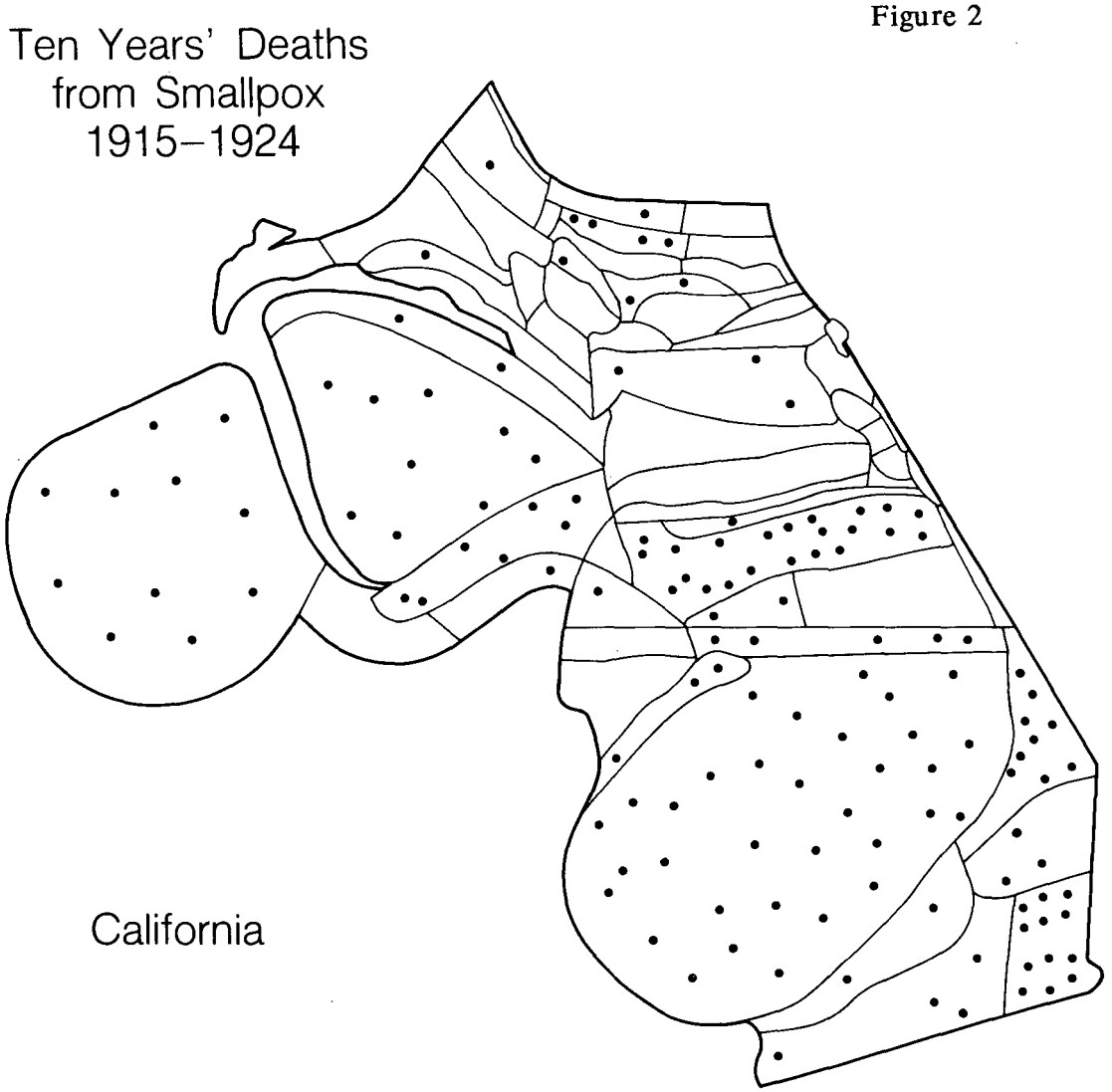

XBL 871-9807

Figure 3

A Transformation (radial): Simplest Case

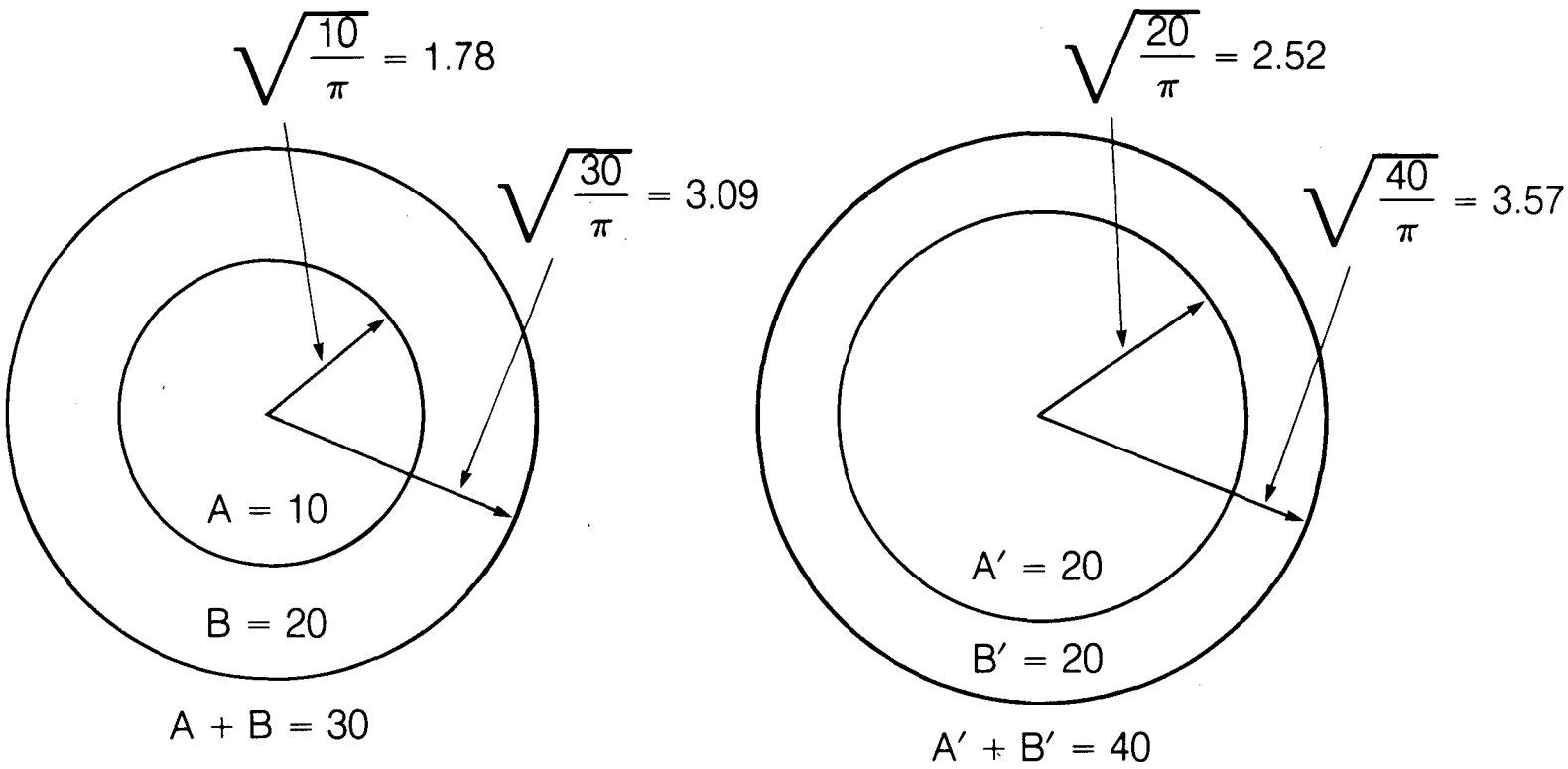

XBL 849-8745A

Figure 4

$$A = \frac{1}{2} R_1^2 \theta \qquad B = \frac{1}{2} R_2^2 \theta - \frac{1}{2} R_1^2 \theta$$

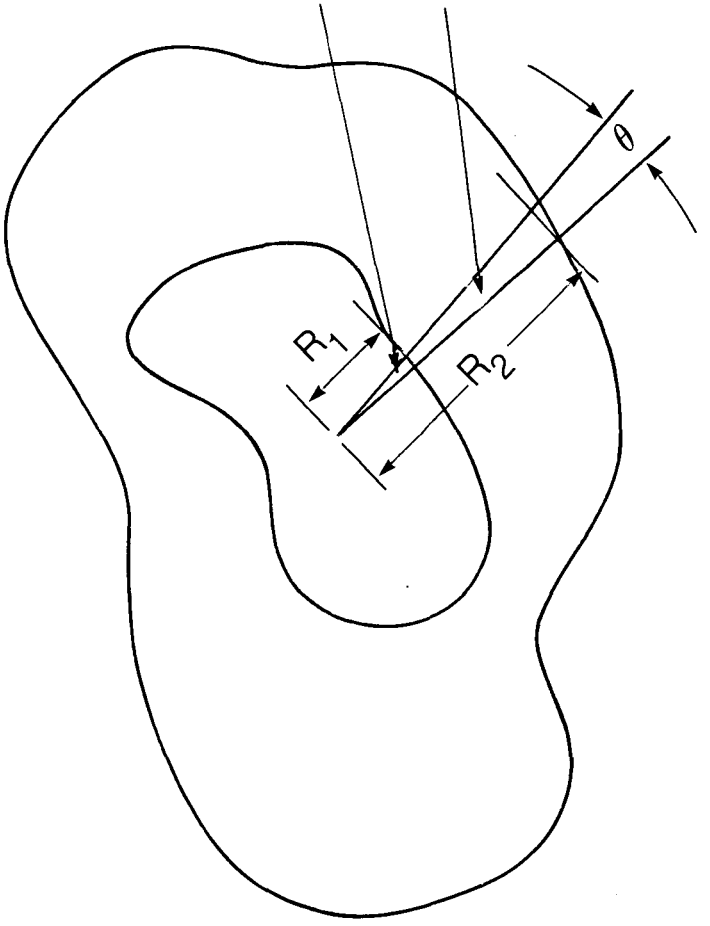

$$B' = B = \frac{1}{2} R_2'^2 \theta - \frac{1}{2} R_1'^2 \theta$$

$$A' = MA = \frac{1}{2} R_1'^2 \theta$$

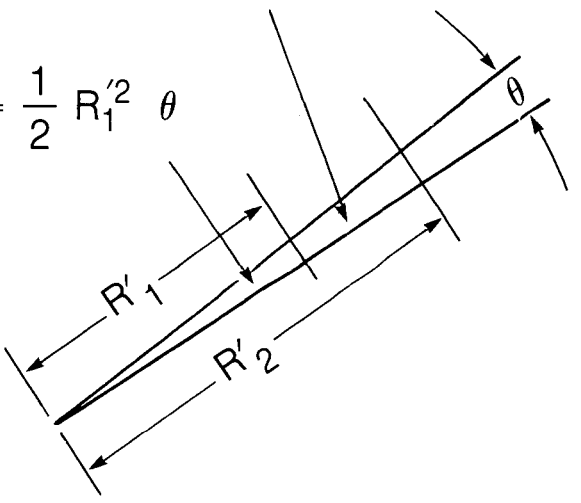

$$R'_1 = \sqrt{M}\ R_1$$

$$R'_2 = \sqrt{R_2^2 + (M-1)R_1^2}$$

XBL 849-8746

Figure 5

Transformed by population — United States

Geopolitical

Transformed

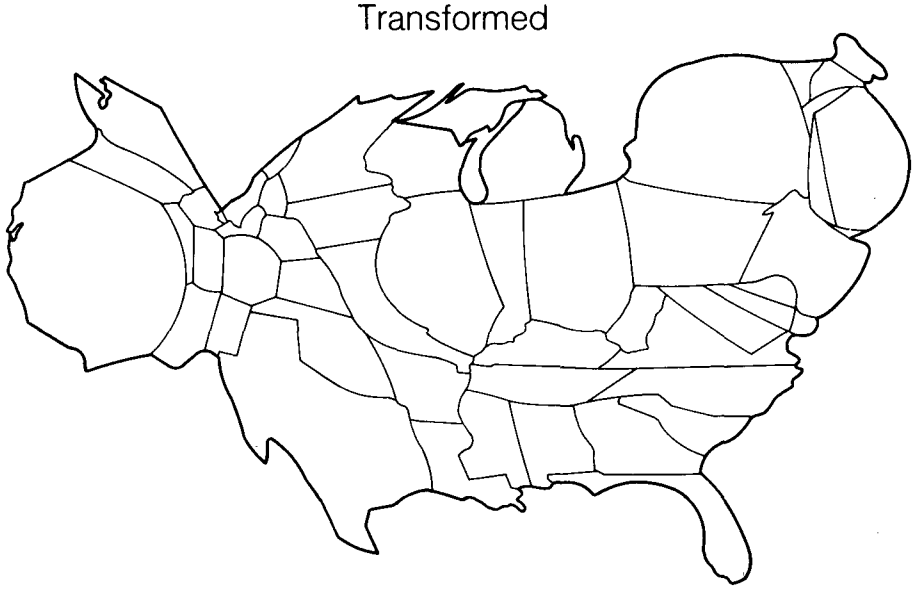

XBL 871-9861

Figure 6

Iowa — Geopolitical

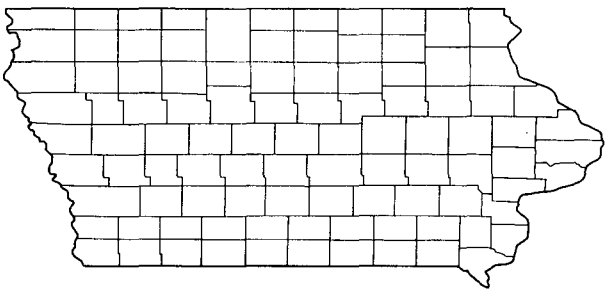

Iowa-Classic Transformation (hand drawn)

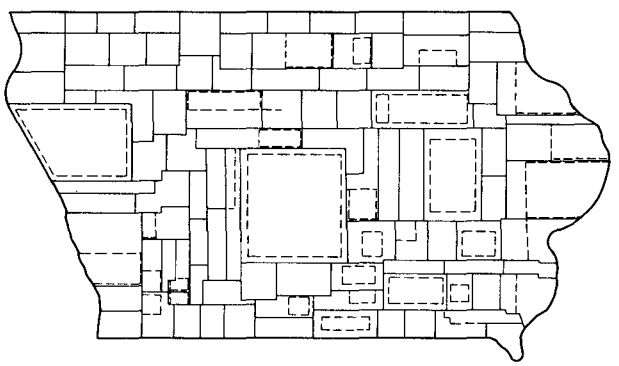

Iowa-Radial Transformation

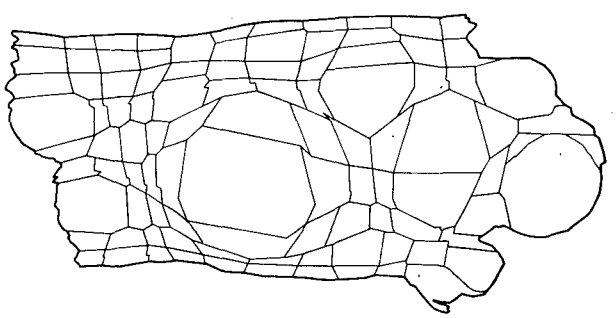

XBL 871-9805

Figure 7

San Francisco — Geopolitical
1980 Census Tracts

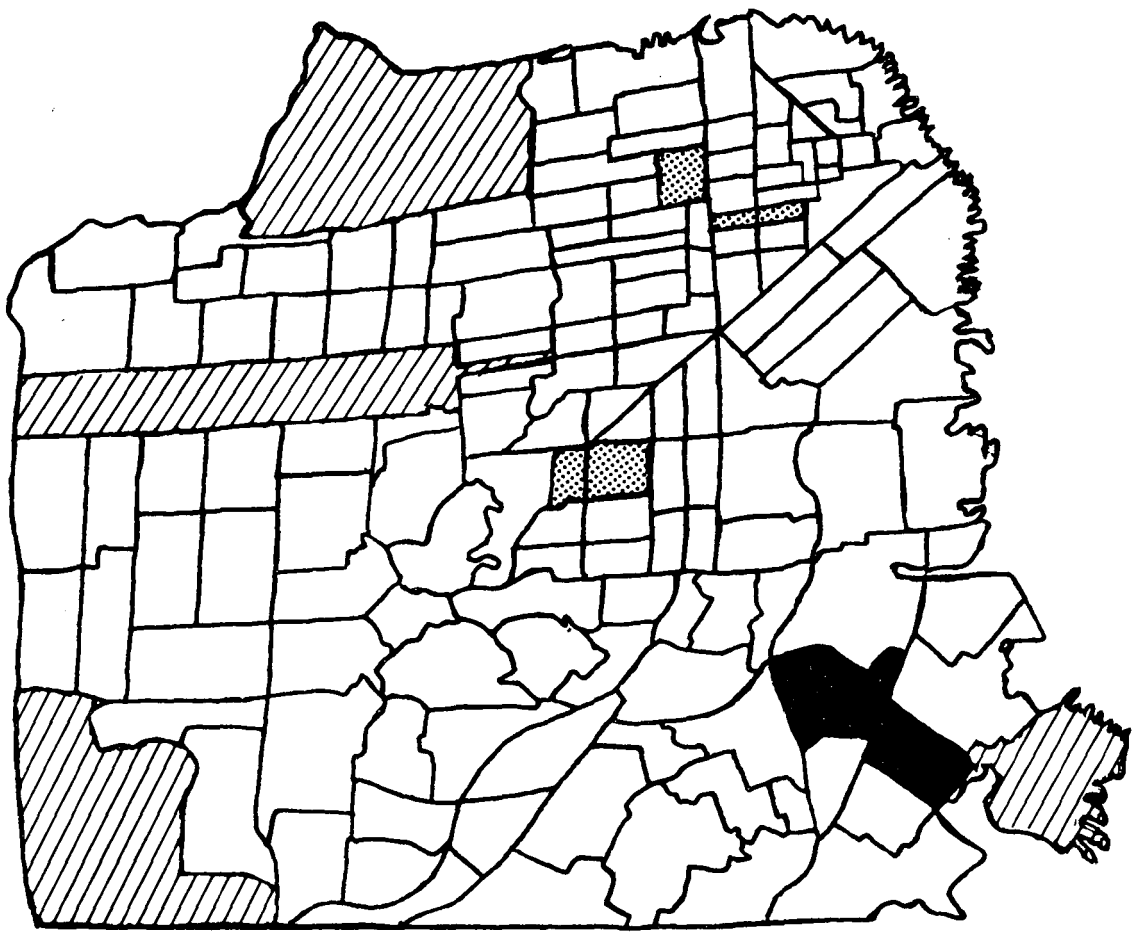

XBL 848-8623A

Figure 8

San Francisco — Transformed
1980 White Male Population
ages 35–54

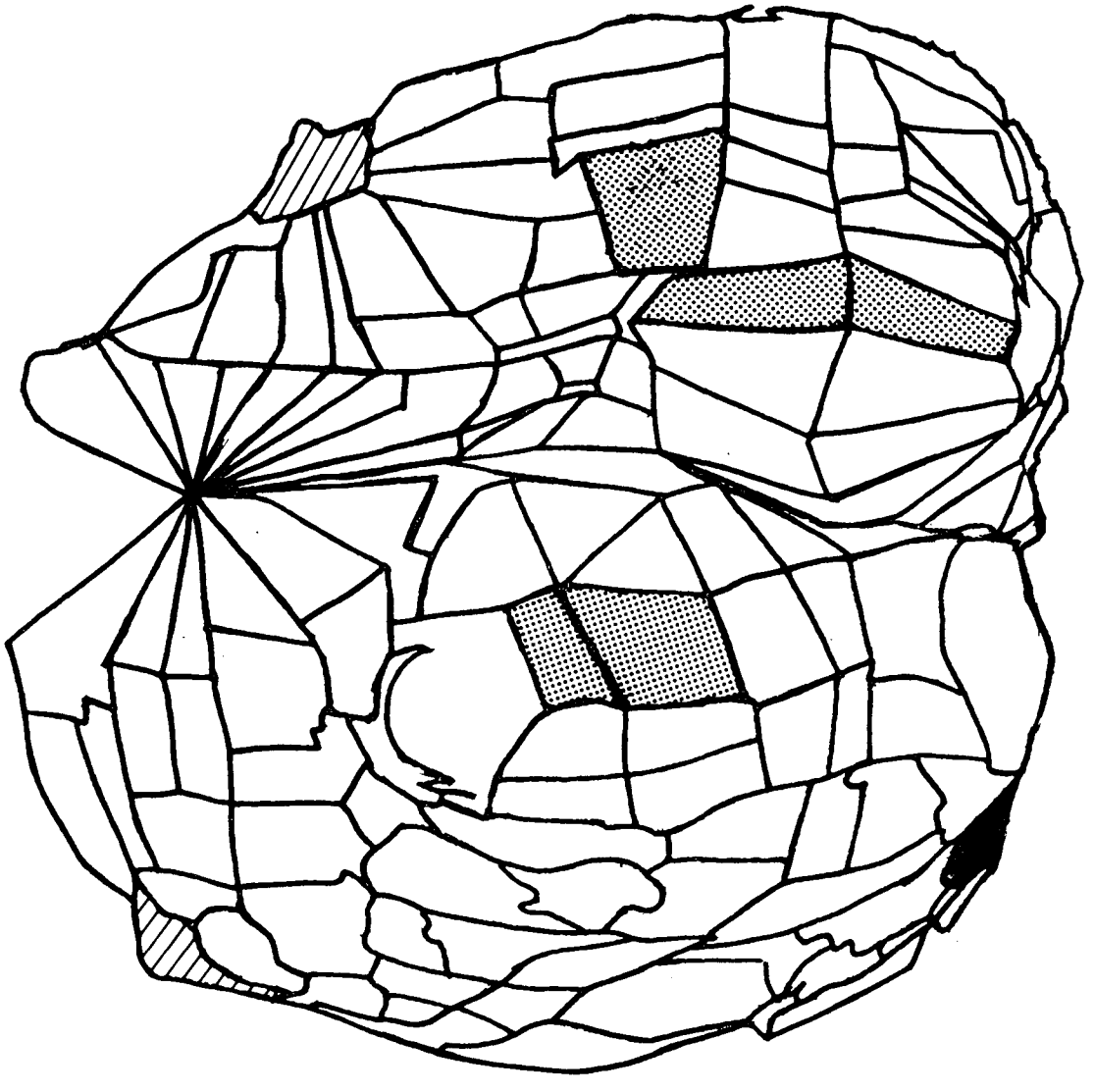

XBL 848-8624A

Figure 9

San Francisco — Transformed
1980 Black Male Population
ages 35–54

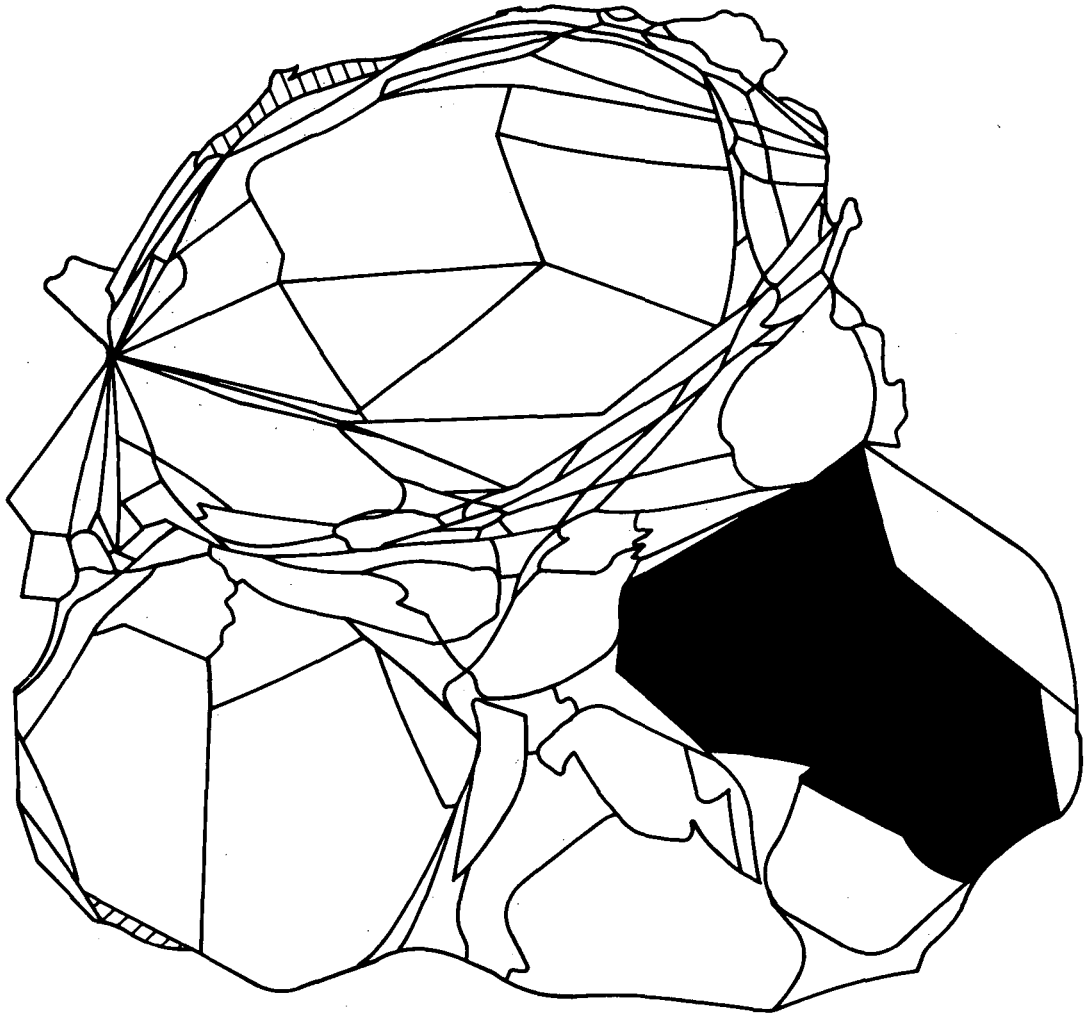

XBL 871-9862

Figure 10

Hypothetical Cases (n = 13)
Non-transformed San Francisco map

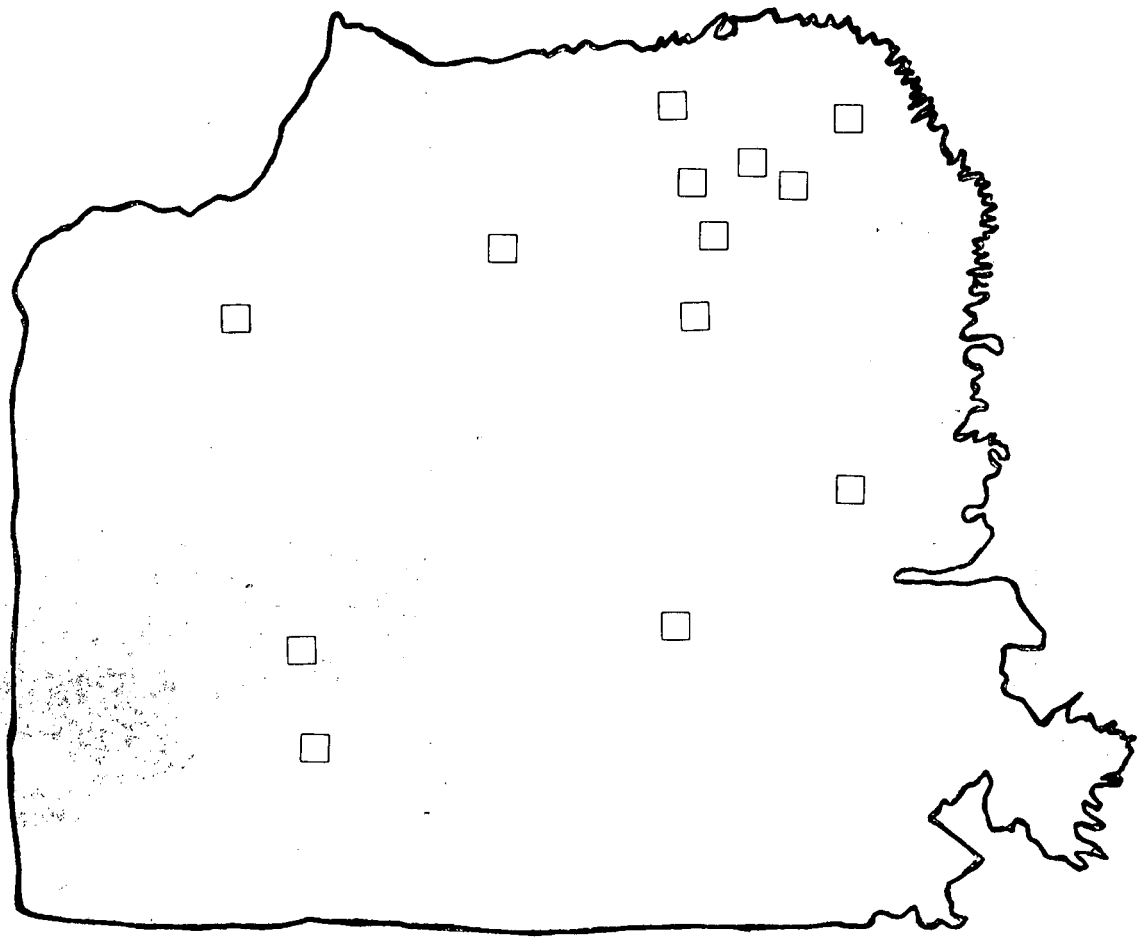

XBL 848-8626A

Figure 11

Hypothetical Cases (n = 13)
Transformed San Francisco map

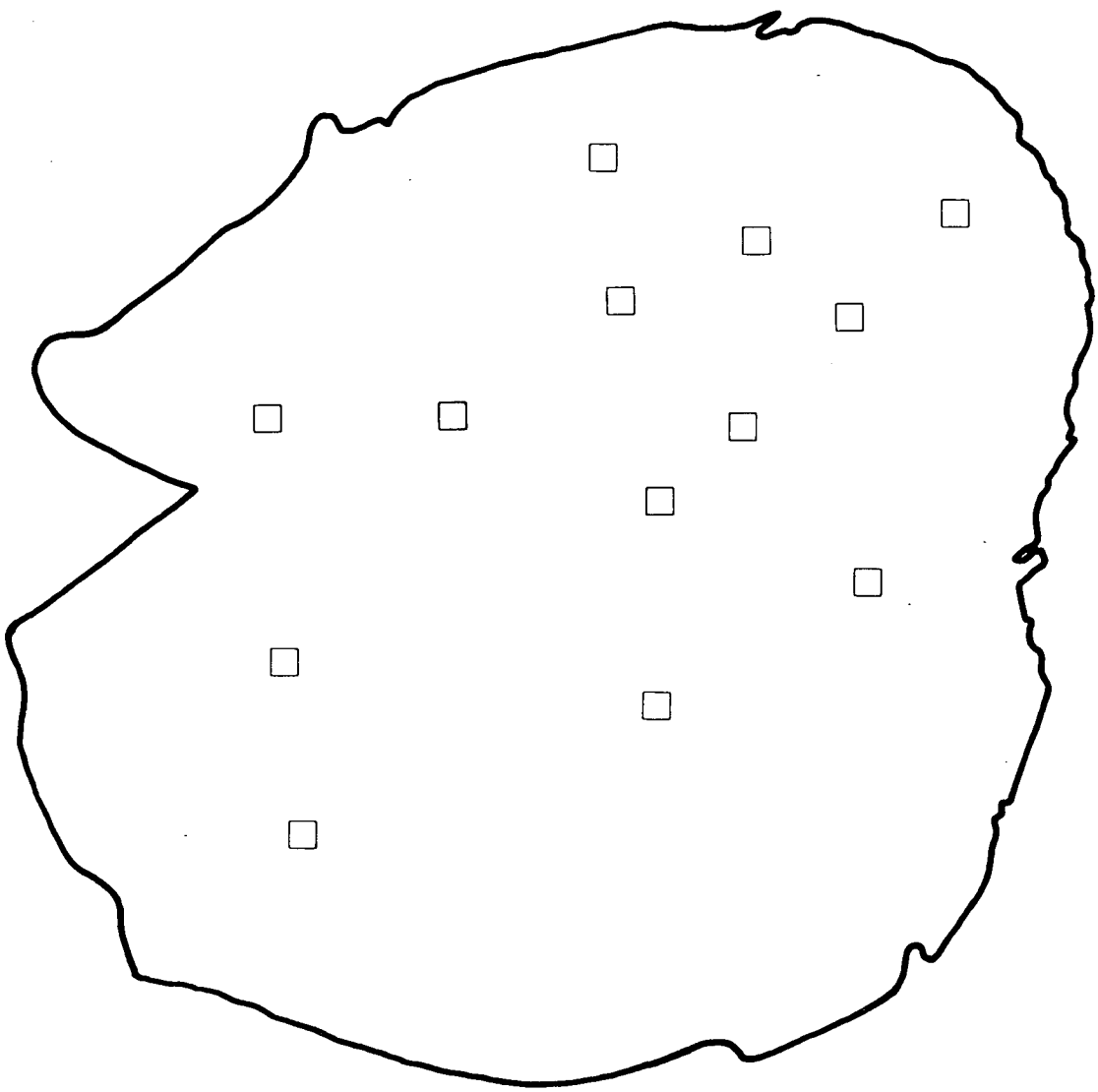

XBL 848-8627A

Figure 12

Colon Cancer
White Females, ages 35 – 54
San Francisco, 1978 – 81

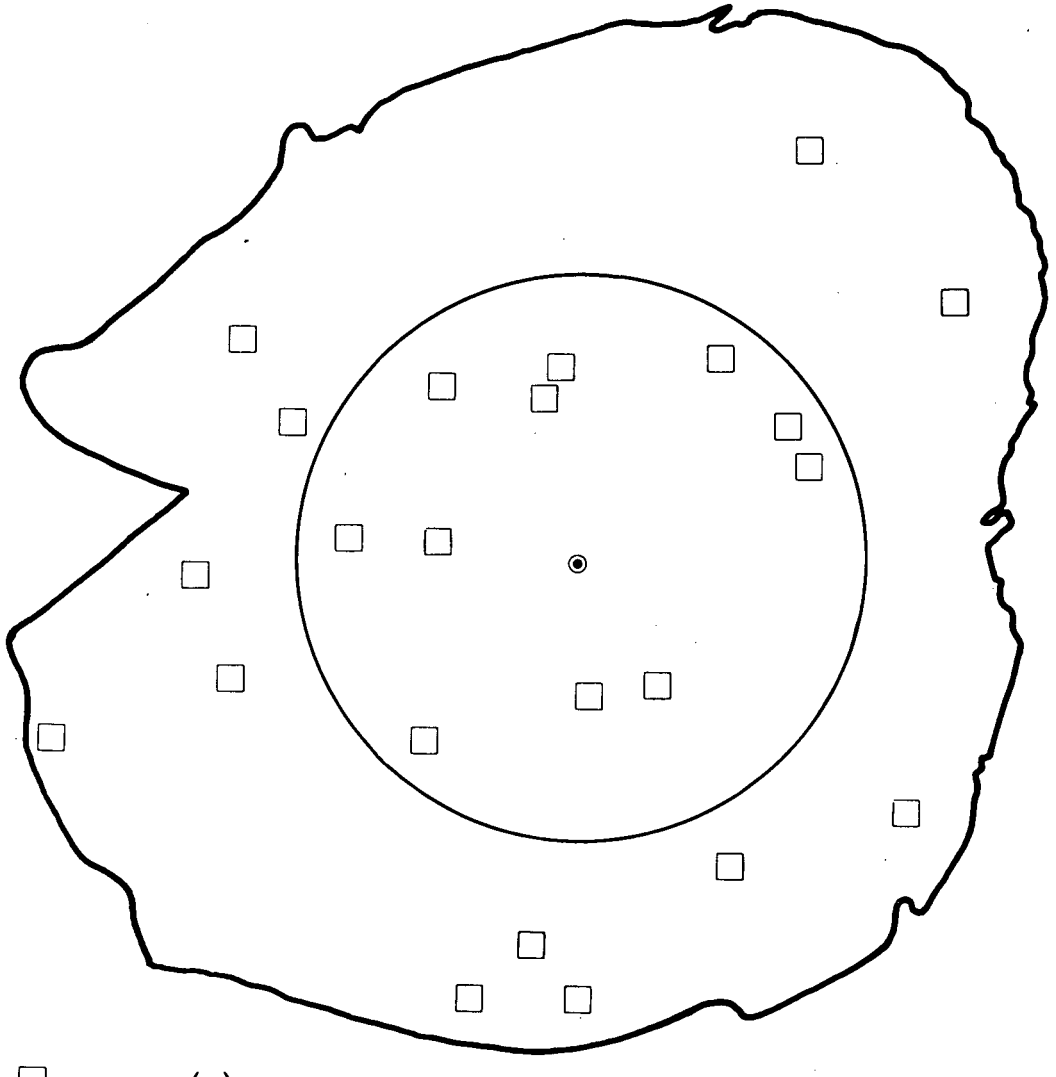

□ = case(s)
◉ = centroid of cases

XBL 848-8630A

Figure 13

Stomach Cancer
White Females, ages 35 – 54
San Francisco, 1978 – 81

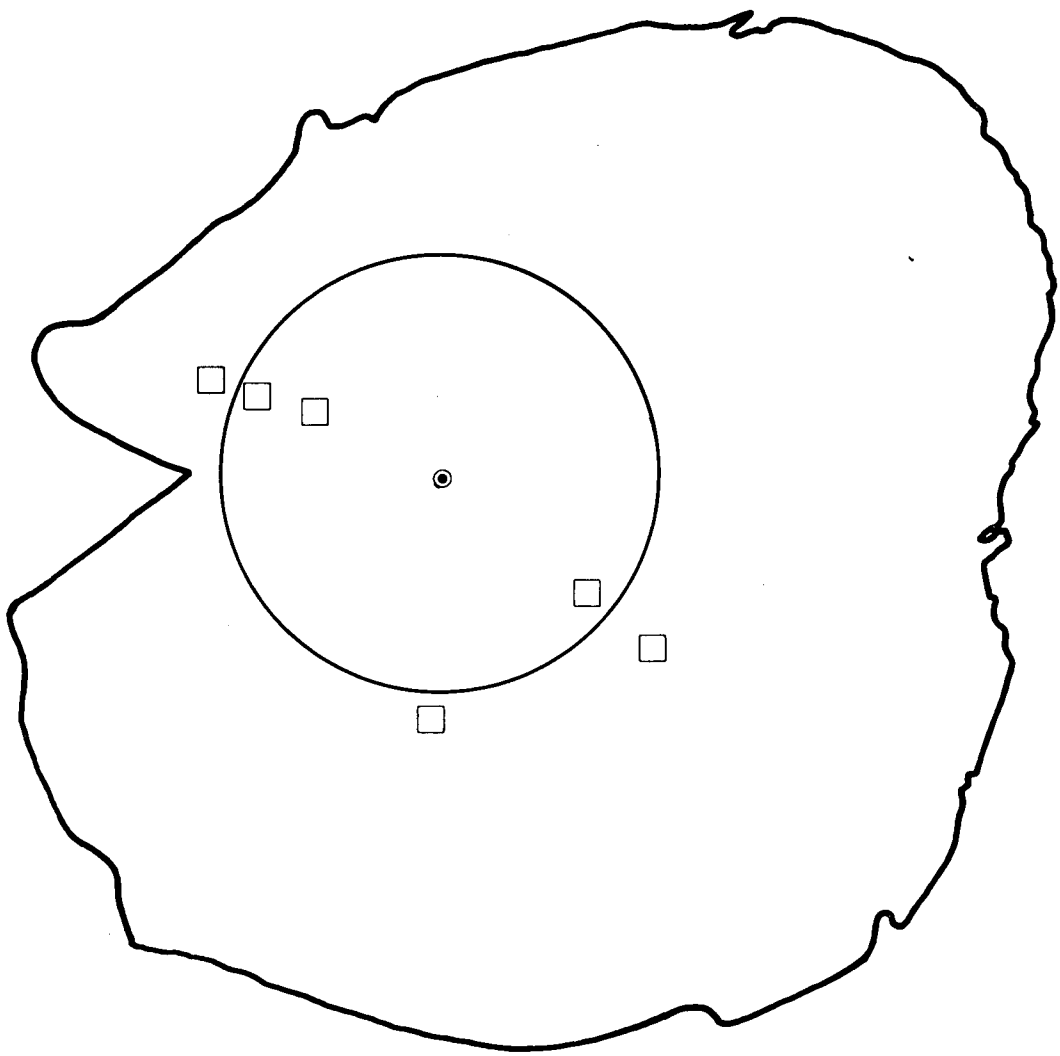

□ = case(s)
⊙ = centroid of cases

XBL 848-8629A

Figure 14

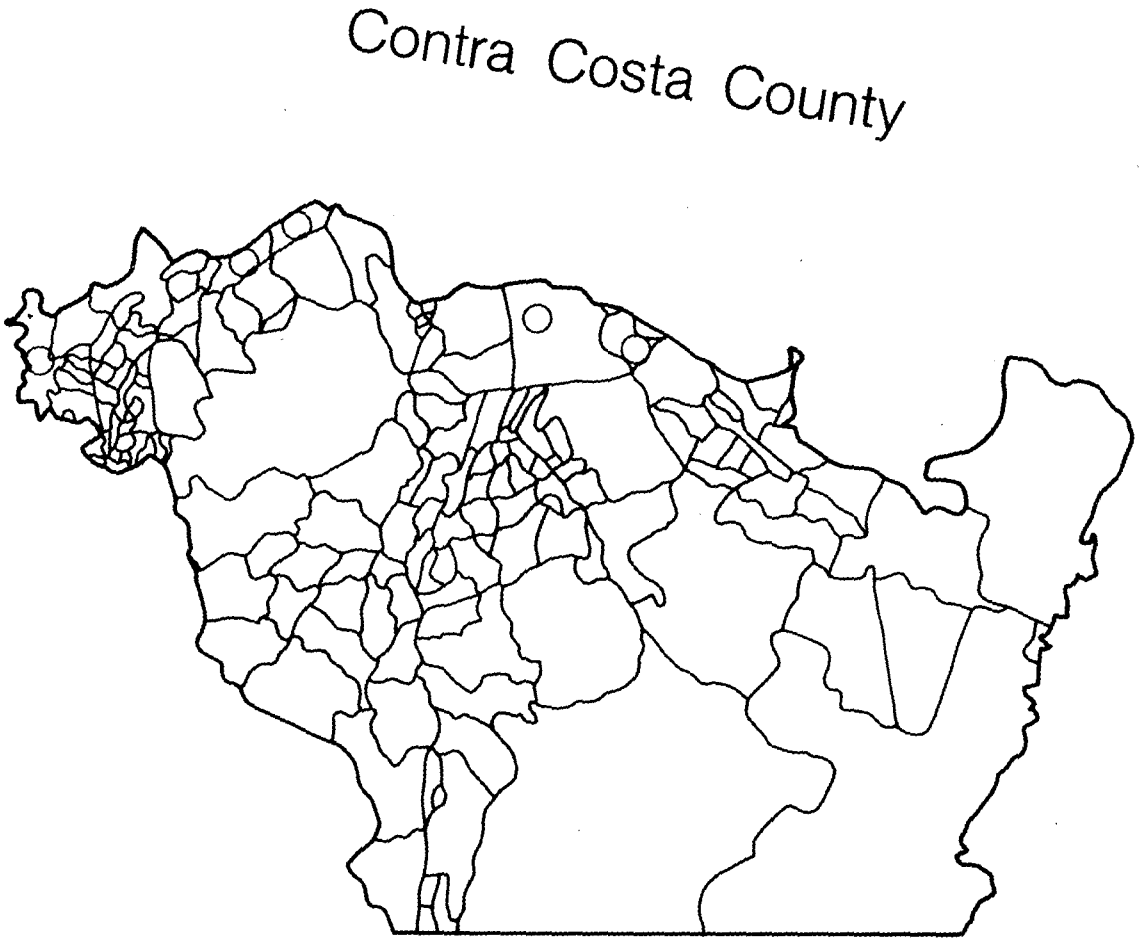

XBL 871-9863

Figure 15

Contra Costa County

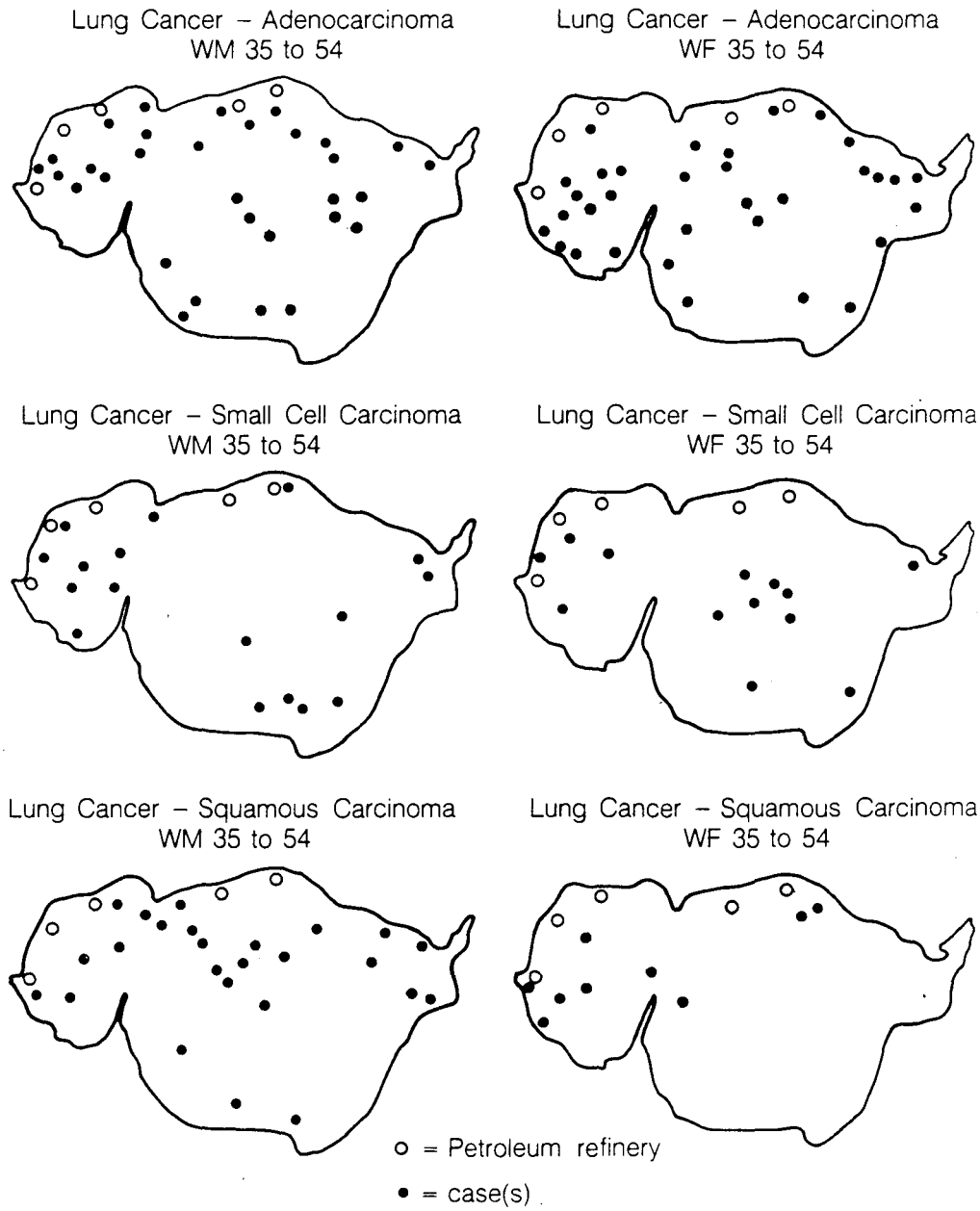

Figure 16

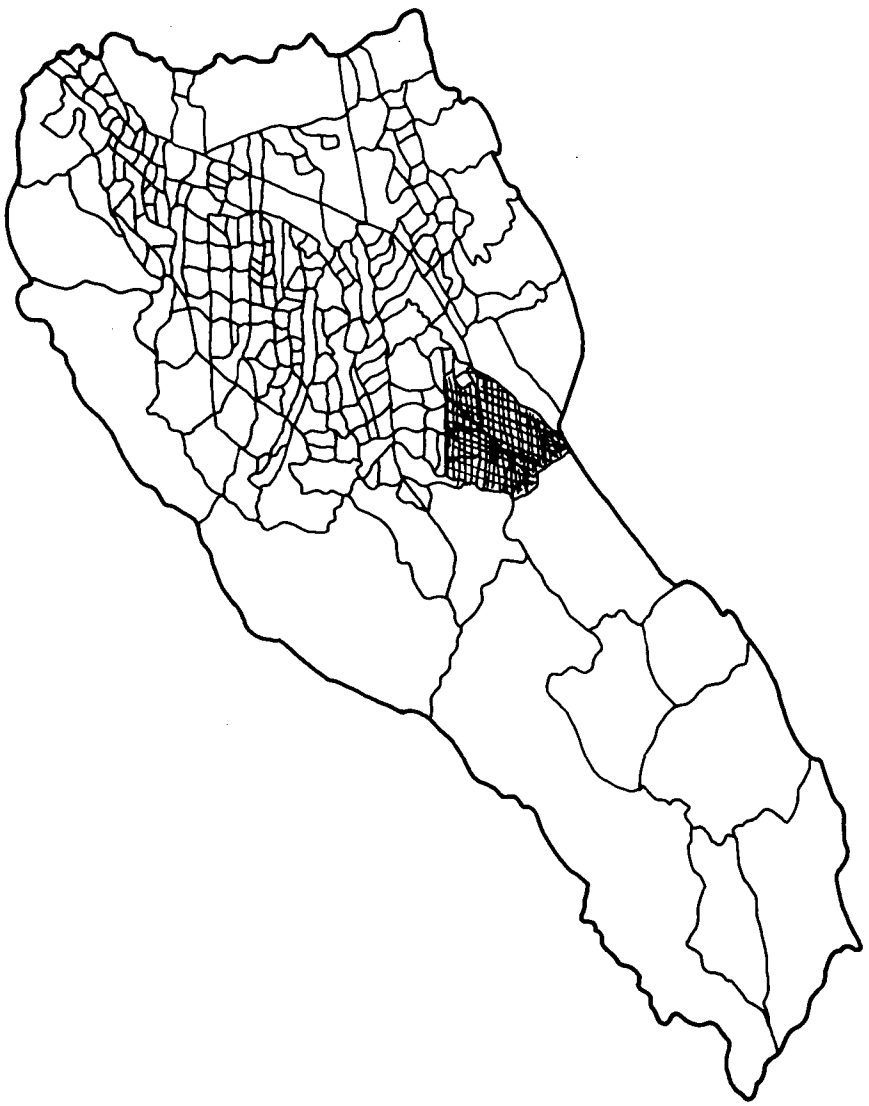

XBL 871-9864

Figure 17

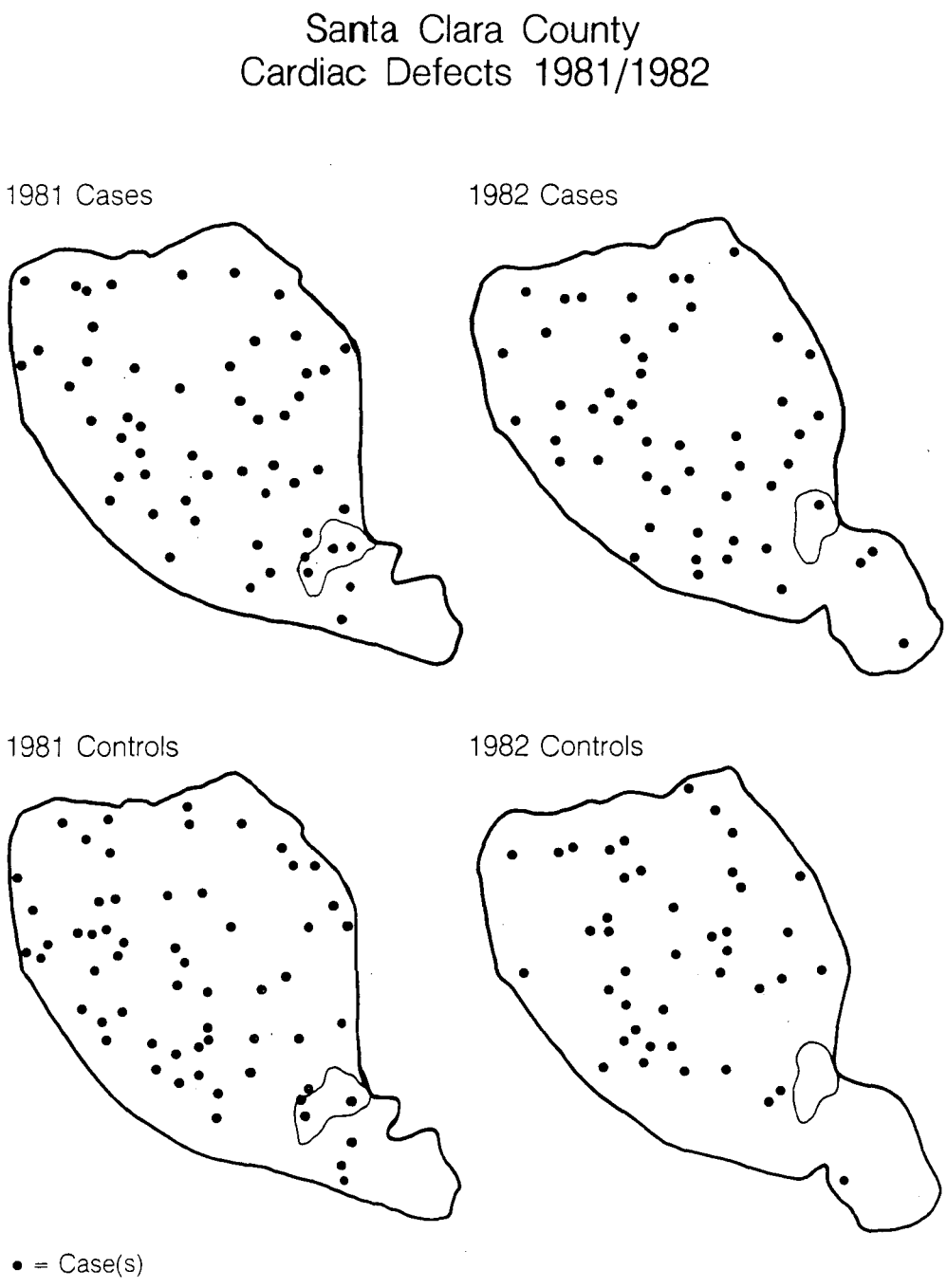
Santa Clara County
Cardiac Defects 1981/1982
1981 Cases
1982 Cases
1981 Controls
1982 Controls
• = Case(s)
XBL 863-9786

Figure 18

Santa Clara County

Cardiac defects 1981

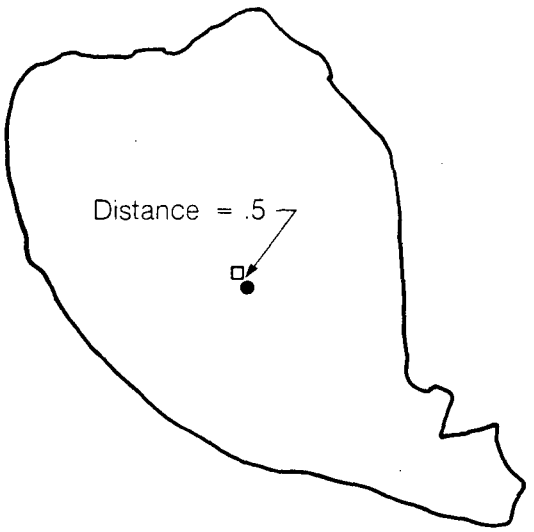

Cardiac defects 1982

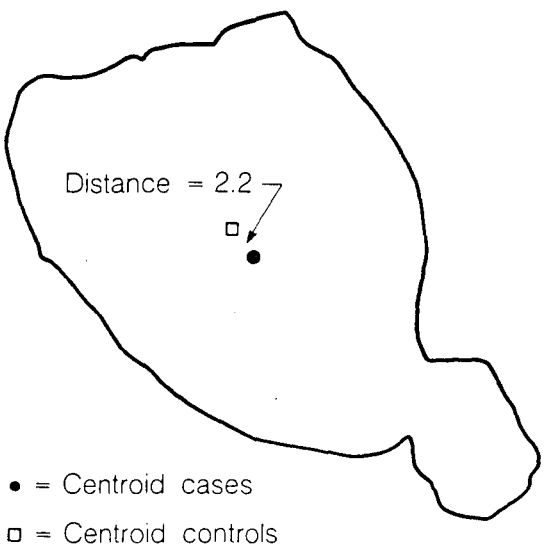

XBL 863-9787

Figure 19

Jefferson/Denver Counties
Colorado

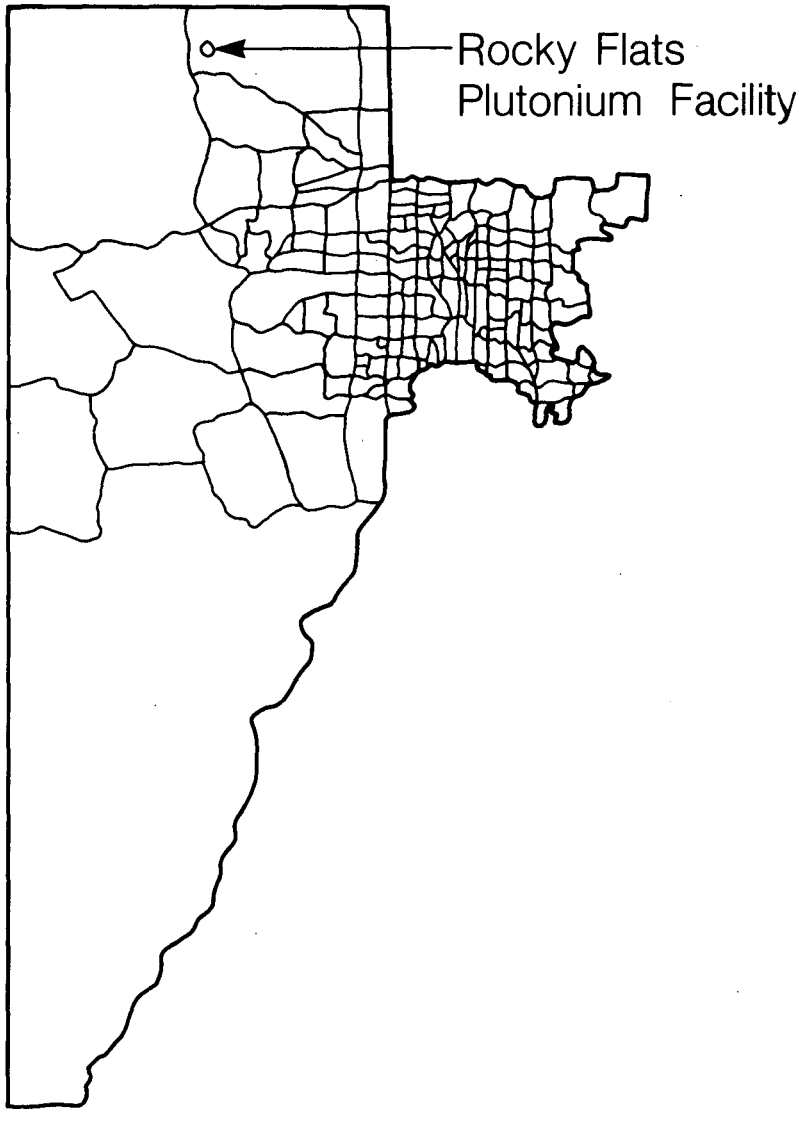

XBL 871-9865

Jefferson/Denver Counties
Colorado

Figure 20

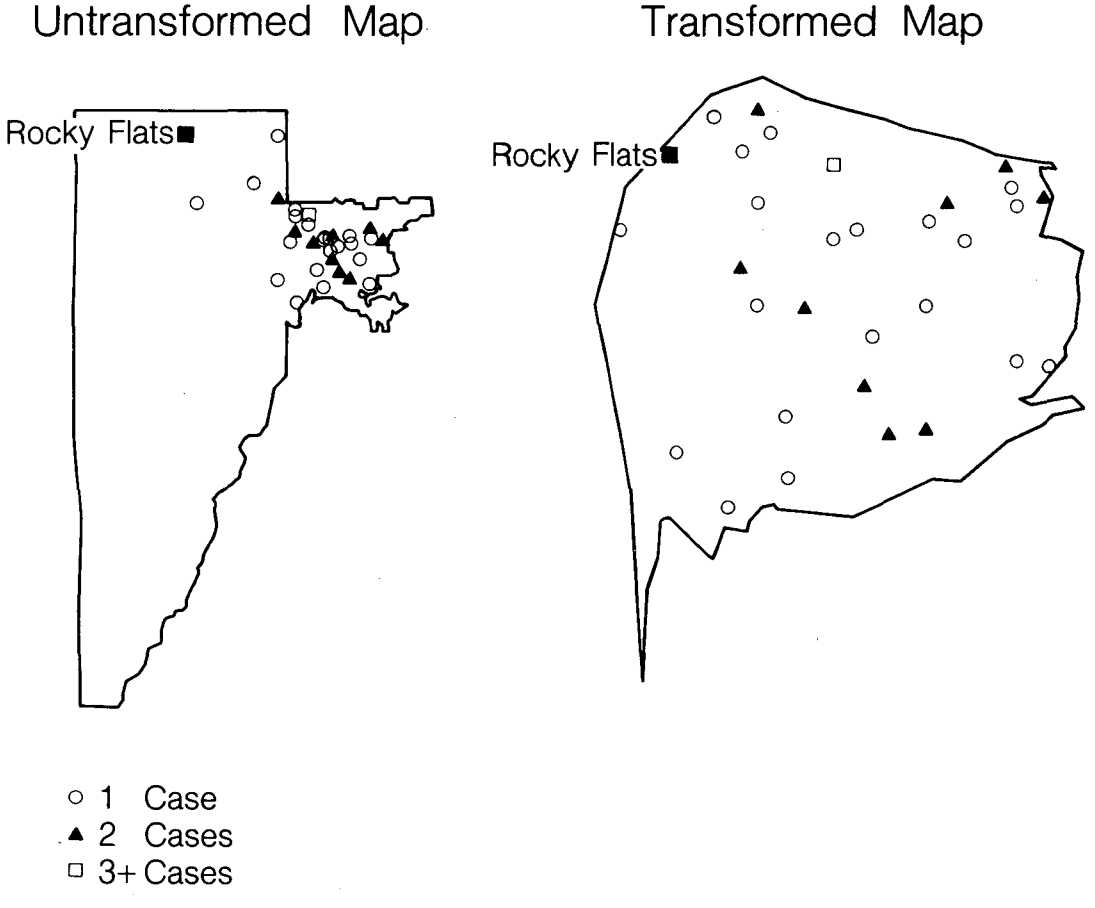

XBL 869-10978A

Figure 21

Lung Cancer (Adenocarcinoma)
White Females 55 +
Jefferson/Denver 1970

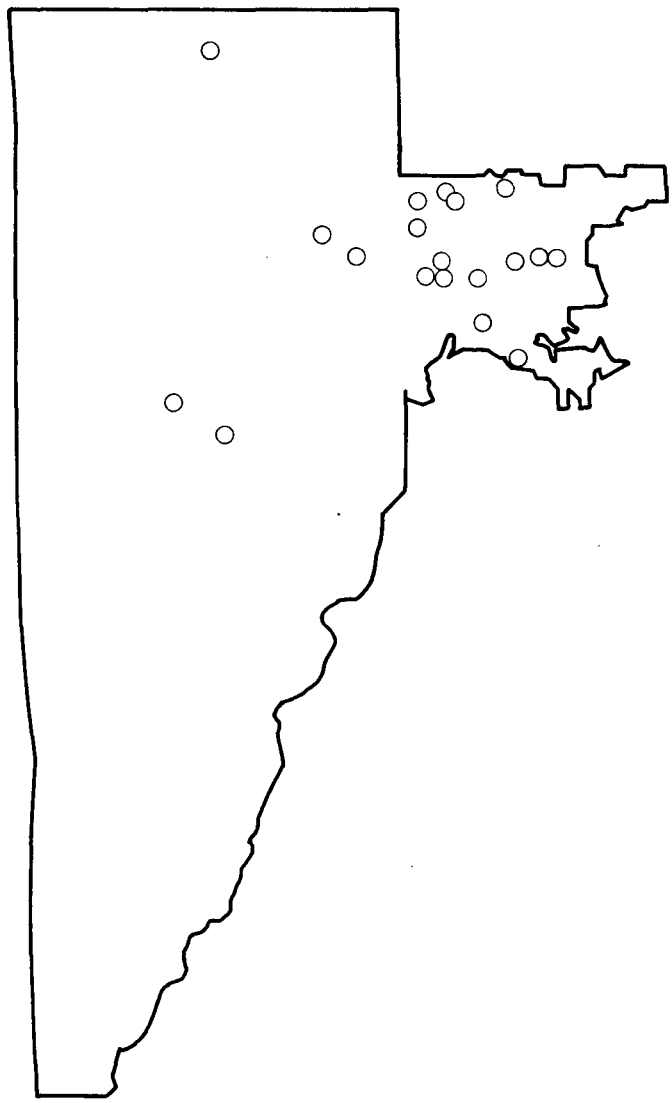

XBL 871-9866

Figure 22

Lung Cancer (Adenocarcinoma)
White Females 55 +
Jefferson/Denver 1970

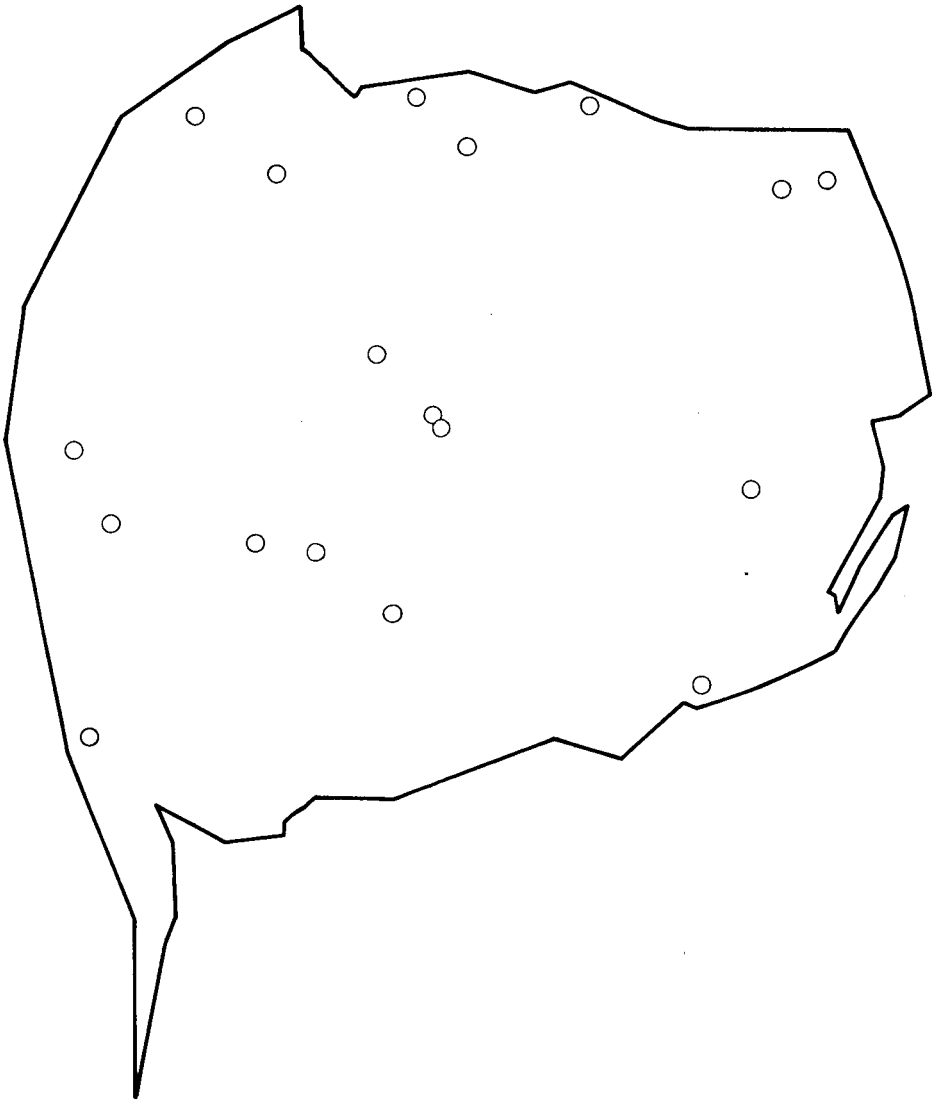

XBL 871-9867

Figure 23

Lung Cancer (Small cell)
White Females 55 +
Jefferson/Denver 1970

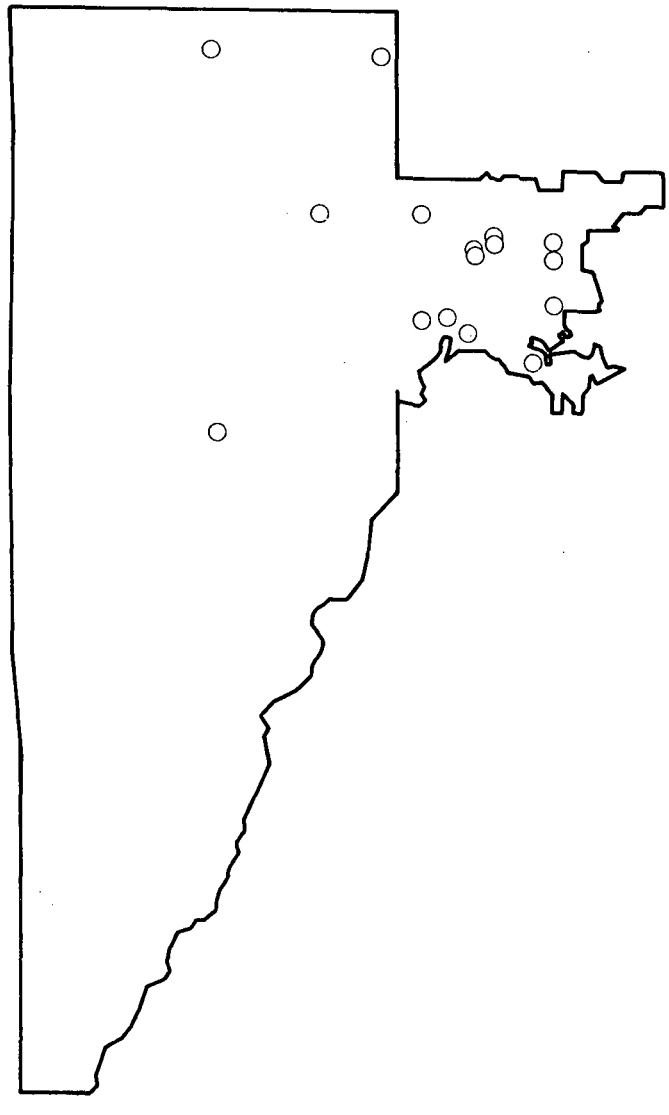

XBL 871-9868

Figure 24

Lung Cancer (Small cell)
White Females 55 +
Jefferson/Denver 1970

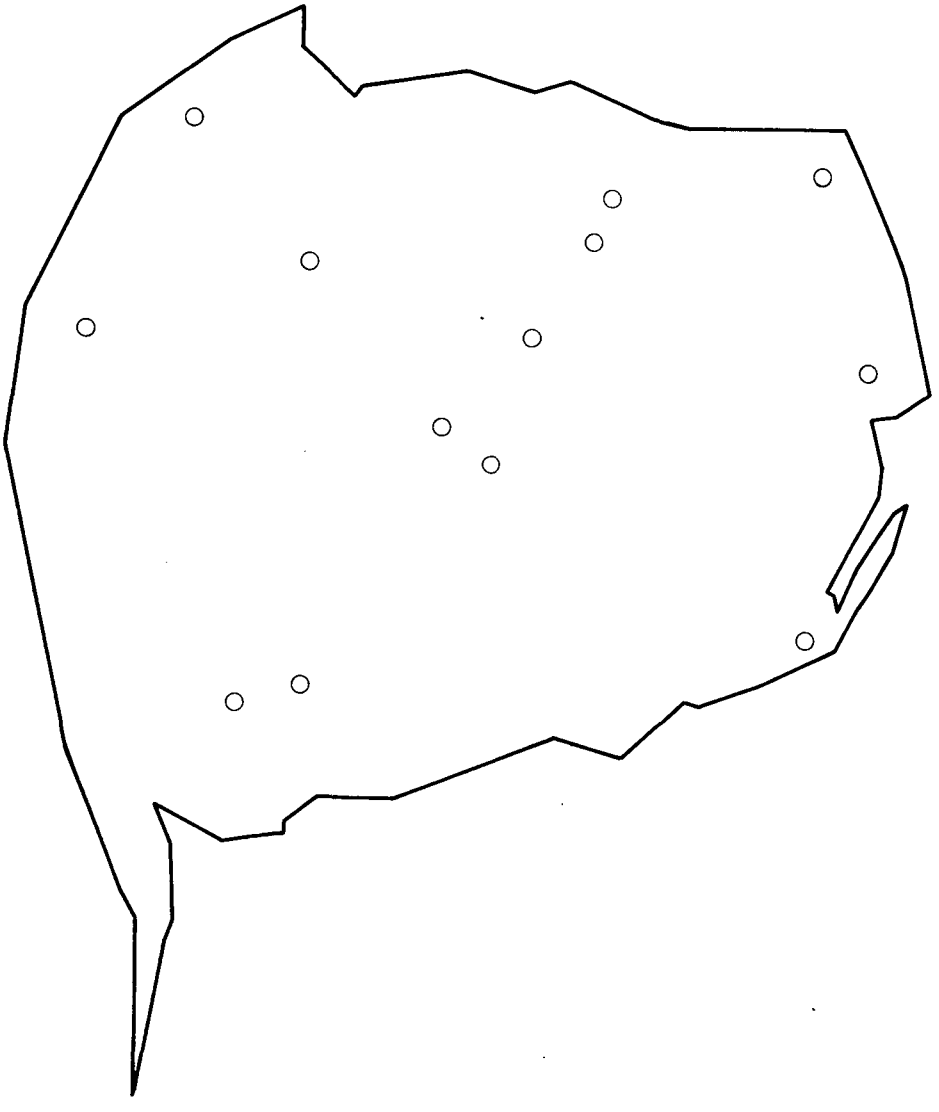

XBL 871-9869

Figure 25

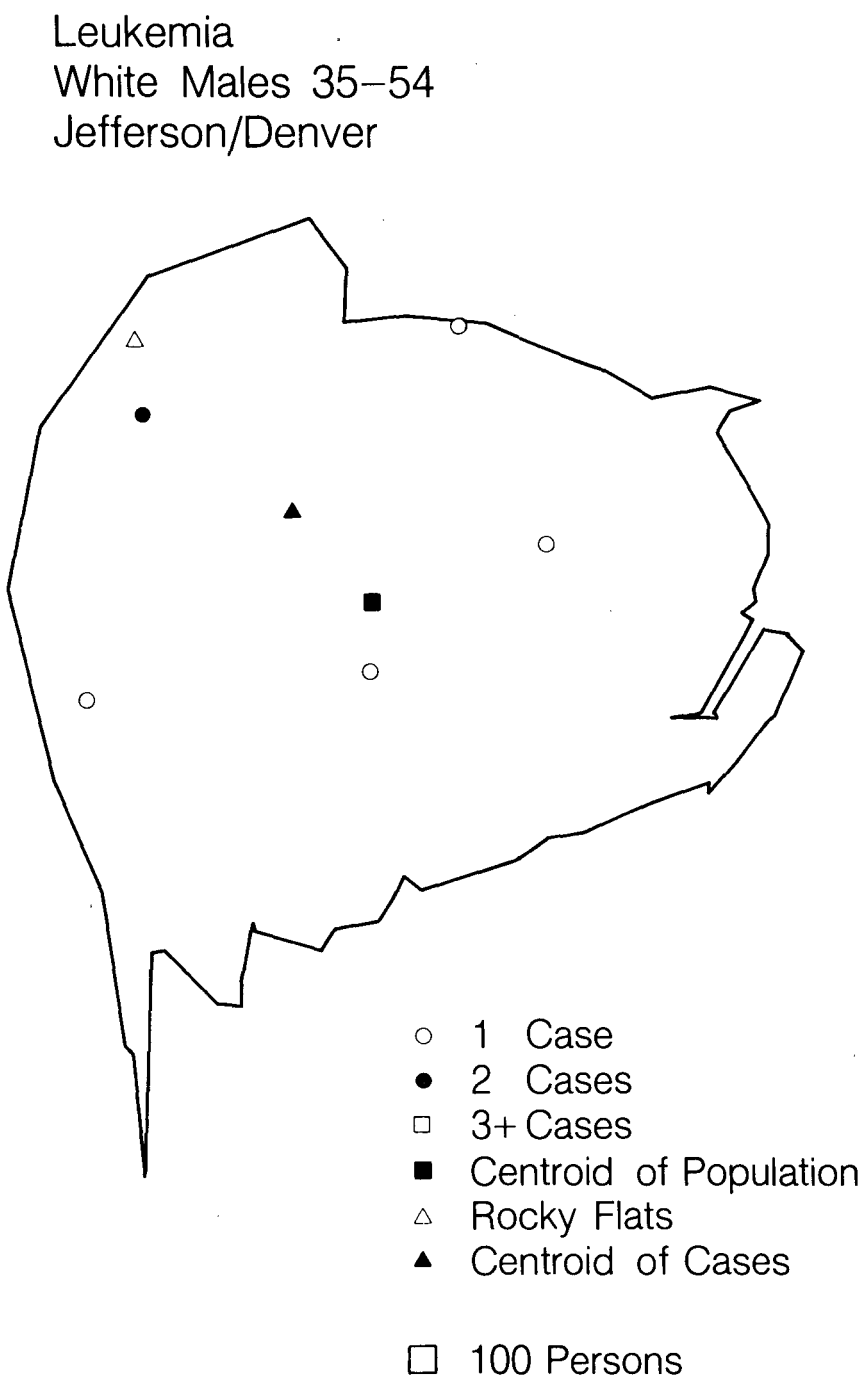

XBL 871-9870

Figure 26

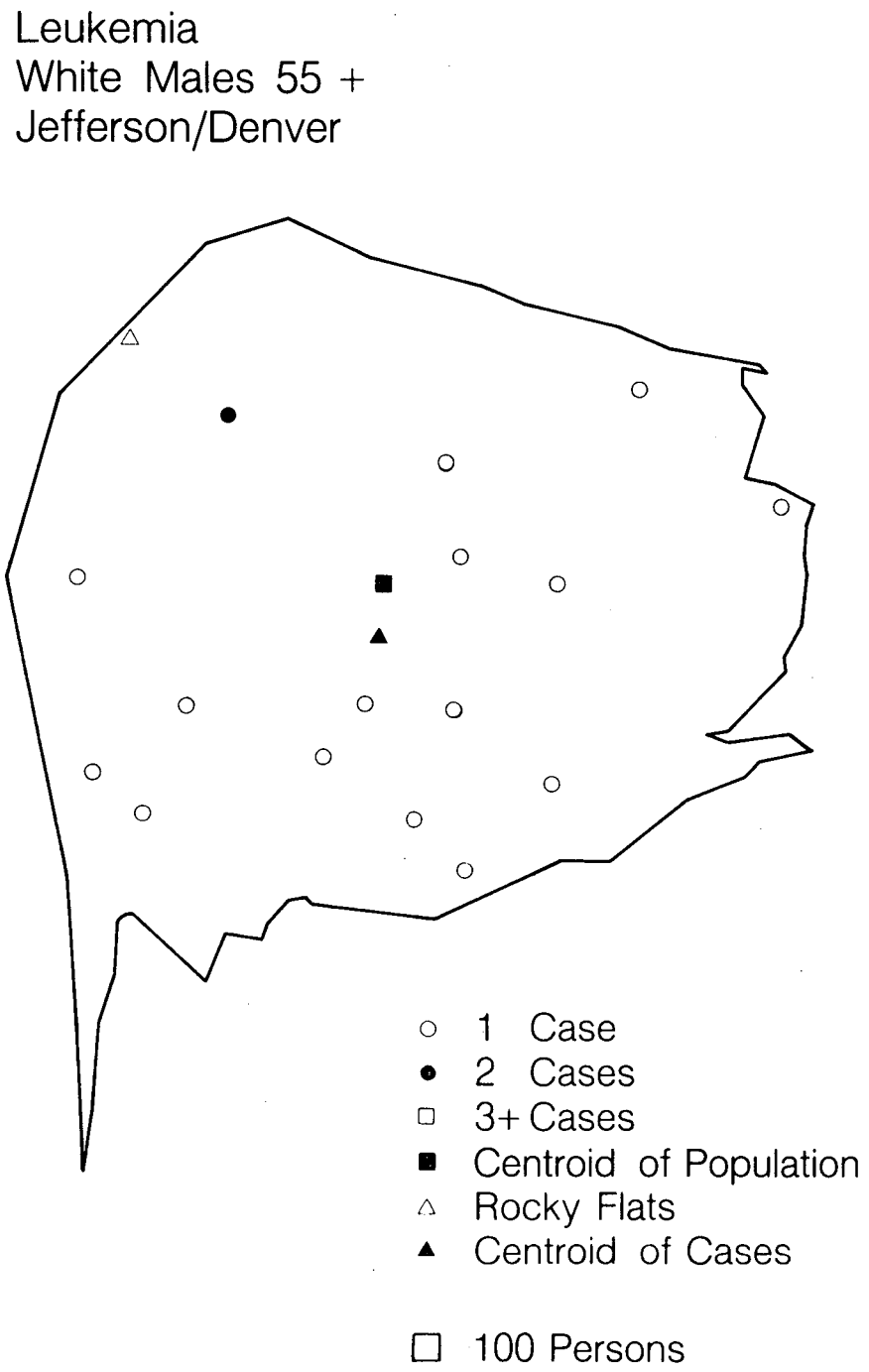

XBL 871-9871

Figure 27

Leukemia
White Females 35–54
Jefferson/Denver

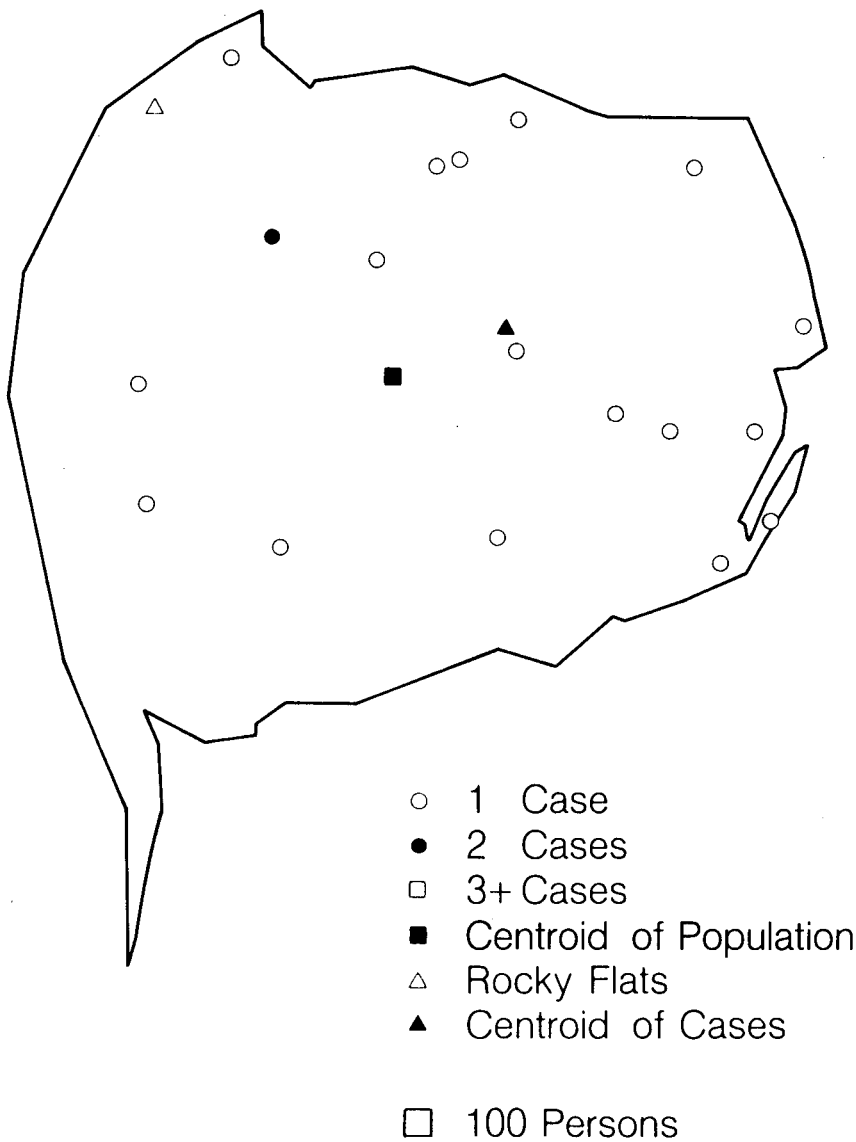

XBL 871-9872

Figure 28

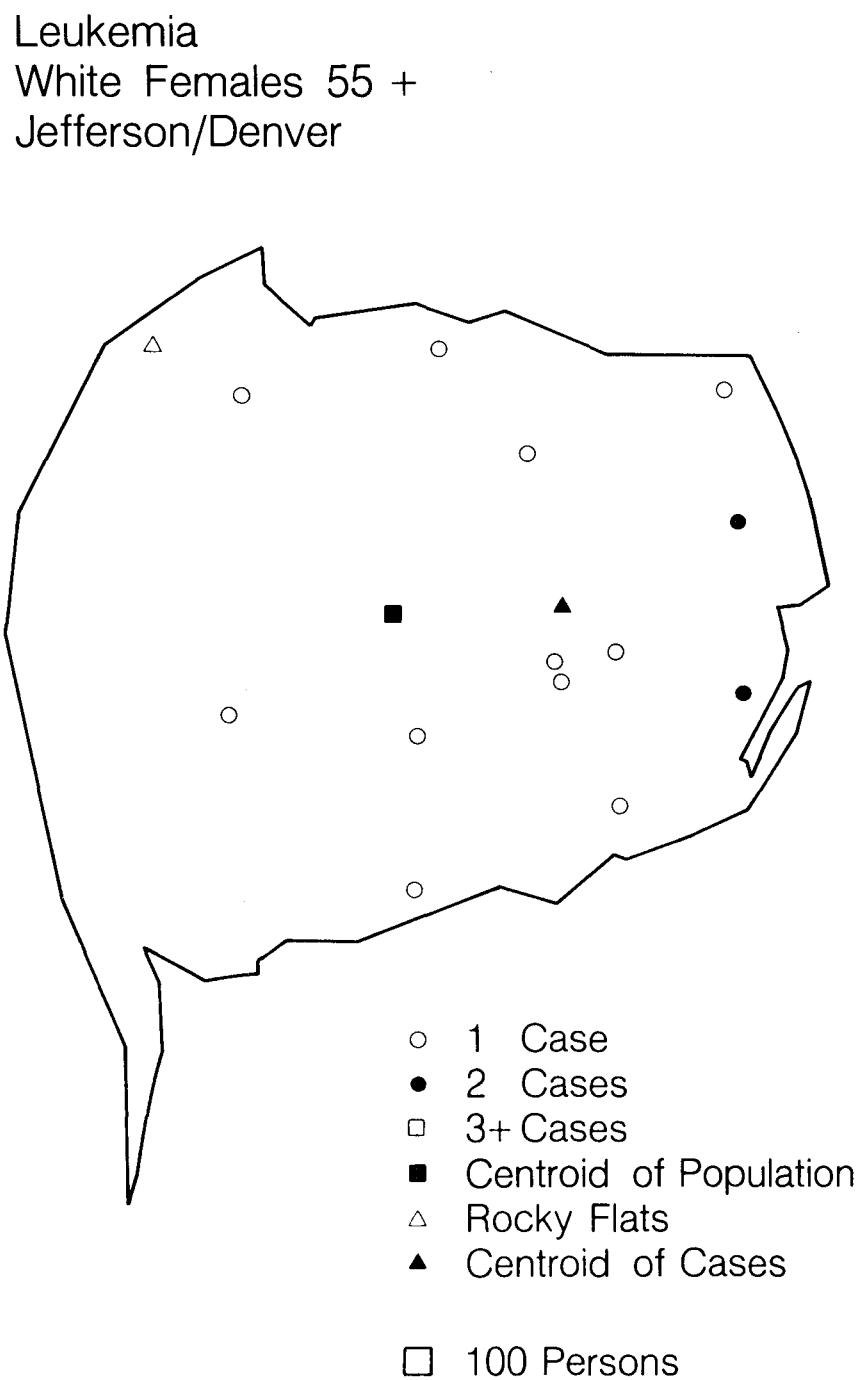

XBL 871-9873

Figure 29

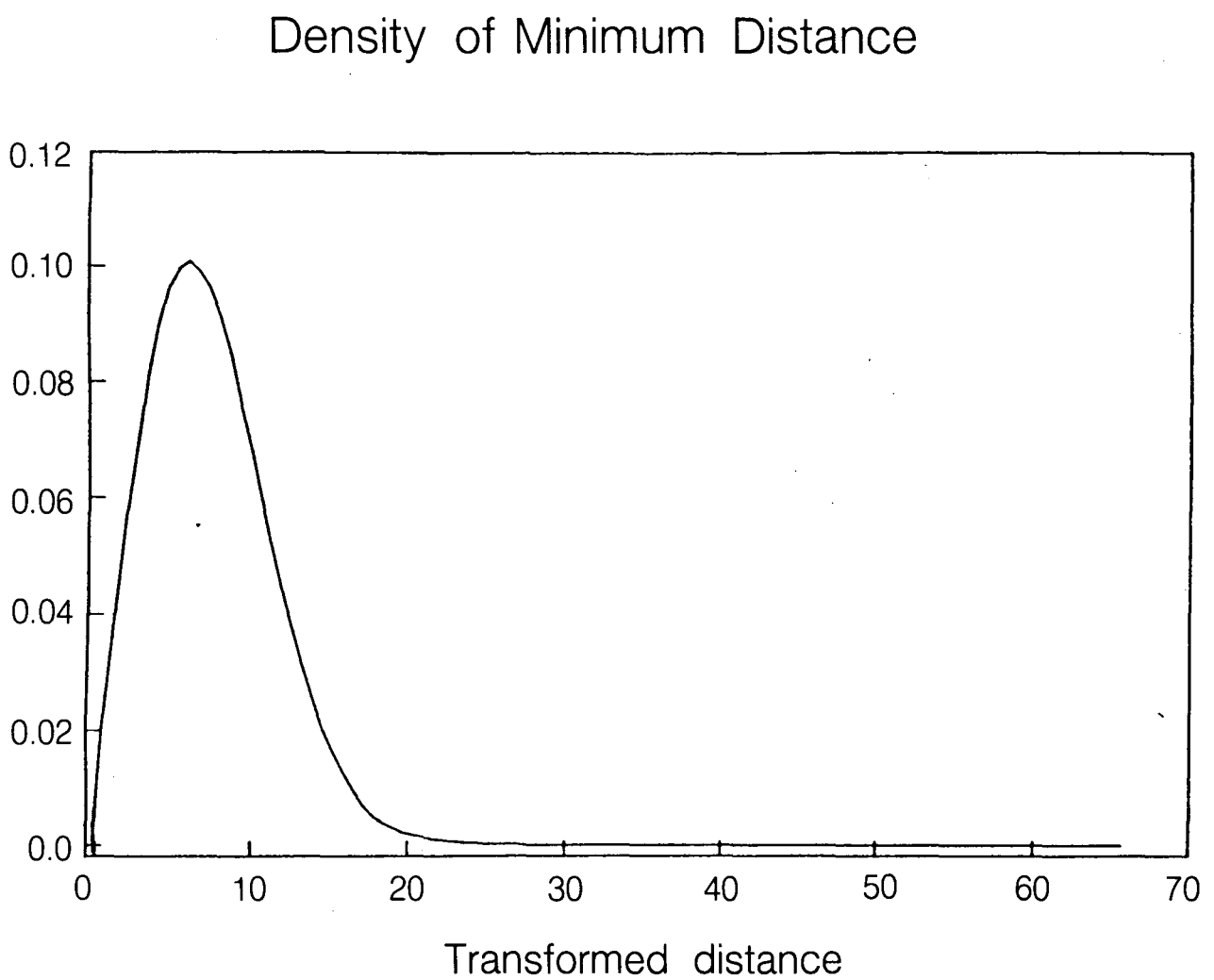

XBL 869-10979A

Figure 30

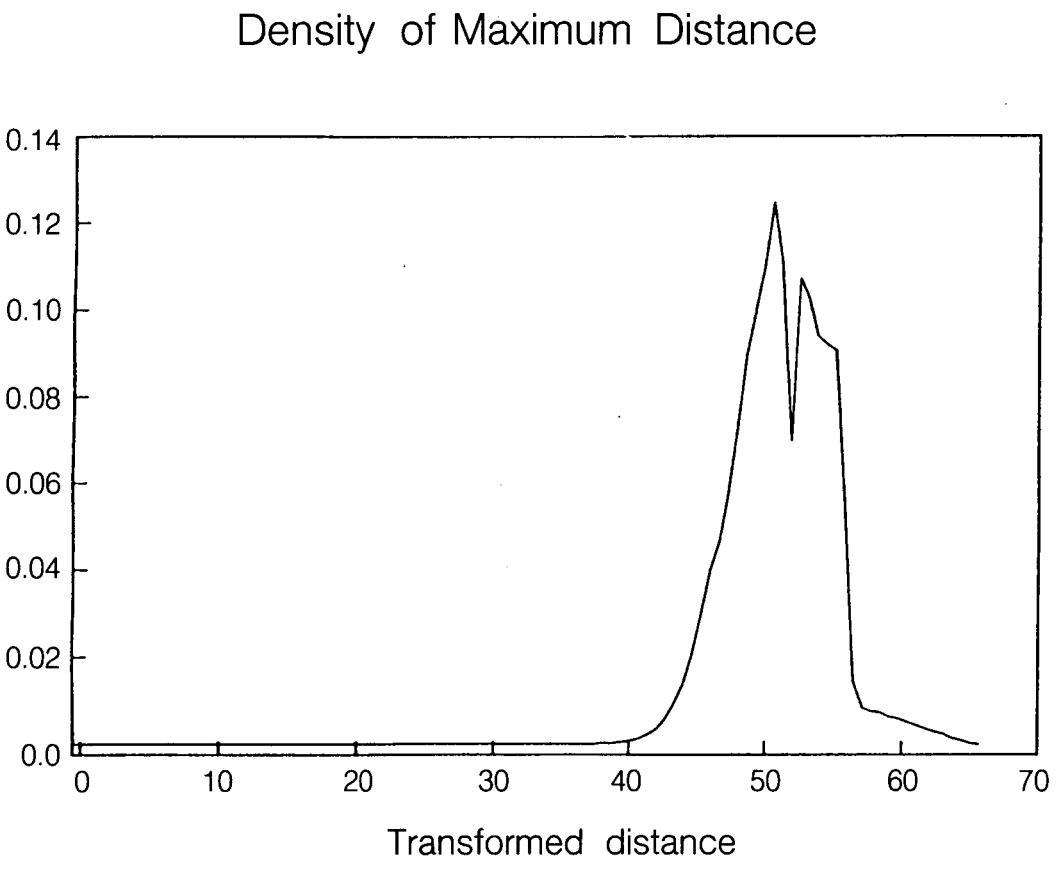

XBL 869-10980A

This report was done with support from the Department of Energy. Any conclusions or opinions expressed in this report represent solely those of the author(s) and not necessarily those of The Regents of the University of California, the Lawrence Berkeley Laboratory or the Department of Energy.

Reference to a company or product name does not imply approval or recommendation of the product by the University of California or the U.S. Department of Energy to the exclusion of others that may be suitable.

LAWRENCE BERKELEY LABORATORY
TECHNICAL INFORMATION DEPARTMENT
UNIVERSITY OF CALIFORNIA
BERKELEY, CALIFORNIA 94720